THESIS

FLOW DURATION CURVES AND SEDIMENT YIELD ESTIMATION FOR URBANIZING WATERSHEDS

Submitted by

Tyler Thomas Rosburg

Department of Civil and Environmental Engineering

In partial fulfillment of the requirements

For the Degree of Master of Science

Colorado State University

Fort Collins, Colorado

Summer 2015

Master's Committee:

Advisor: Peter A. Nelson
Co-Advisor: Brian P. Bledsoe

Ellen E. Wohl

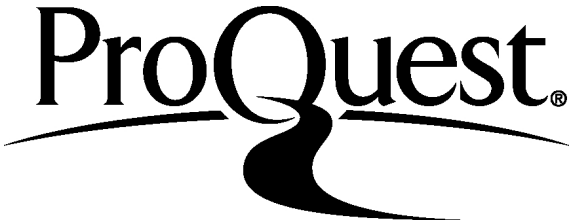

ABSTRACT

FLOW DURATION CURVES AND SEDIMENT YIELD ESTIMATION FOR URBANIZING WATERSHEDS

Land use change associated with urbanization can alter natural flow regimes, typically resulting in larger peak flows for a given precipitation event than in a pre-urbanized watershed condition. The overall influence of urbanization on how flows of different frequencies might change over time, while important in hydrologic design, remains poorly understood. In this study, we first investigate the effects of urbanization on flow duration curves (FDCs) and flow variability through a case study of several watersheds in the Puget Sound Region of Washington State.

A FDC is a graphical representation of the frequency, or fraction of time, that a discharge magnitude is equaled or exceeded. Using different time windows of the flow record, we analyzed stream discharge, precipitation, and watershed urbanization for a minimum of 25 years between 1960 and 2010 to quantify how key FDC percentiles changed with time in response to urbanization in small watersheds (less than 200 km^2) with land uses ranging from highly urban to primarily rural. In the urban watersheds, the 95^{th}-99^{th} percentile of the daily-mean flow series increased by 0-94% with an average increase of 35%. The magnitude of small discharges (10^{th} percentile) in the urban watersheds also increased by up to 34% with an average increase of 15%. The rapidity and magnitude of changes in streamflow, commonly known as “flashiness,” was also observed to increase over the period analyzed for both urban and rural watersheds.

Flashiness increased by 46% on average in urban watersheds, a result likely caused by increases in population density and impervious surfaces. Rural watersheds were found to have lesser increases in flashiness, 14% on average, attributed to baseflow reductions and increasing precipitation intensity and variability.

As watersheds become flashier, the decision to use either daily-averaged or sub-daily streamflow records has the potential to impact the calculation of sediment transport metrics. To investigate, we calculated the effective discharge, sediment yield, and half-load discharge using sediment rating curves over long time periods with both daily-averaged and sub-daily streamflow records, in the second part of this study. The pool of sites in the analysis included 39 sites with bedload measurements and 99 sites with suspended load measurements from several regions of the United States. Results of this analysis were compared to site-specific metrics such as stream flashiness and bed sediment size. A comparison of sediment transport metrics calculated with both daily-average and sub-daily stream flow data at each site showed that daily-averaged flow data were unable to adequately represent the magnitude of high streamflows at flashy sites. This caused an underestimation of sediment transport and sediment yield at flashy sites, the degree of which was controlled by the magnitude of the best-fit exponent of the sediment rating curve. Regression equations are provided for estimating this bias as a function of stream flashiness and sediment rating curve parameters. No relationship between flow data resolution and effective discharge was found. The results of this analysis help inform the use of FDCs and sediment yield estimation in urbanizing watersheds. This analysis demonstrates the magnitude of change that urbanization may cause in a FDC. Additionally, this analysis illustrates the importance of using sub-daily flow data in the calculation of sediment yield in urbanizing or otherwise flashy watersheds.

ACKNOWLEDGEMENTS

I would first like to thank my academic advisers, Dr. Peter Nelson and Dr. Brian Bledsoe for giving me the opportunity to work on this project. Their continual guidance and support was instrumental to me in the research process. Dr. Nelson and Dr. Bledsoe also provided editorial support that greatly improved this paper. I would also like to thank Dr. Ellen Wohl for her feedback and assistance with my thesis. A special thank you goes to Joel Sholtes for sharing his sediment transport data with me and for his willingness to answer my data analysis questions. This work was funded by the National Cooperative Highway Research Program. I am grateful for their support.

I would also like to thank my family for their support and for instilling the importance of education in me from an early age. Lastly, and most importantly, I would like to thank my wonderful wife Laura. Without her love and support, my dream of earning this degree would not have been possible. Laura provided me with continual encouragement throughout this process. I love you Laura!

TABLE OF CONTENTS

LIST OF TABLES

LIST OF FIGURES

1. CHAPTER 1: INTRODUCTION

As human populations grow, watersheds around the world are responding to urbanization, a diverse collection of influences that cause fundamental changes in watershed hydrologic processes. Hallmarks of urban areas include roads, sidewalks, parking lots, and buildings. These features, which are impervious by nature, alter watershed processes through a number of mechanisms. Impervious surfaces and compacted soils physically limit infiltration of precipitation. This reduces the quantity of water reaching the subsurface and increases surface runoff volume (Booth, 1991). Streets, rooftops, and modern stormwater conveyance systems that collect and funnel stormwater cause runoff to reach streams in a much more rapid fashion than natural overland flow (Leopold, 1968; Putnam, 1972, Boyd et al., 1993); this causes lag time, the duration between the center of mass of rainfall excess and the peak flow rate, to be reduced. As a result of these changes, flow magnitude and frequency are altered.

A flow duration curve (FDC) is a graphic representation of the frequency and magnitude of all instantaneous, daily, weekly, or monthly flows for a given period of time. FDCs have a wide variety of applications including water-use planning, flood mitigation, and reservoir sedimentation studies (Vogel & Fennessey, 1994). FDCs are also critical components of the analysis of magnitude and frequency of sediment transport in rivers. The effective discharge, the discharge that transports more sediment than any other over a period of years (Emmett & Wolman, 2001), is a commonly utilized channel design metric that is typically calculated with a FDC. In regions with coarse-bedded streams and snowmelt hydrology, the effective discharge can be viewed as a reasonable surrogate for the entire series of discharges that form and maintain river channel dimensions (Doyle et al., 2007).

The effects of urbanization on the full spectrum of flow frequencies, and the channel design metrics such as effective discharge that depend on those frequencies, are still not fully understood. It is well known that urbanization causes increases in flood magnitude (Hollis, 1975). Heavily urbanized locations often exhibit flood magnification factors from 2-5, where a flood magnification factor is defined as a factor by which a past design flood quantile would have to be multiplied by to obtain the magnitude of the flood in the current time period (Vogel et al., 2011). This illustrates that urbanization is causing large peak flows to become more common. Urbanization has also been linked to the decline of stream baseflow in certain instances (Price, 2011; Simmons & Reynolds, 1982). Although studies like these have focused on quantifying the effect of urbanization on high and low magnitude discharges, its effect on the full spectrum of flows is less understood. A greater understanding of how urbanization impacts FDCs would be helpful for a number of applications including the estimation of effective discharge and other channel design metrics in urbanizing systems.

Urbanization has also been shown to cause rapid variations in streamflow over short periods of time (Graf, 1977; Walsh et al., 2005). This type of streamflow behavior is termed "flashy" and is also common in small (Ågren et al., 2007) and arid (Allan & Castillo, 2007) catchments. In these types of systems, little is known on how the resolution of streamflow data (daily-averaged or sub-daily) affects the calculation of effective discharge and other sediment yield metrics. A study of six watersheds in East Devon, England showed that sediment yield calculations from daily flow records could vary up to 10% from those made with instantaneous records (Walling, 1977). Additionally, in a study of the Yazoo River basin in Northwest Mississippi, sediment yields created from daily-averaged flow data were 1-100% less than sediment yields created from 15-minute data (Hendon, 1995). However, it is not clear how

flashiness was related to the error in sediment yield calculations for these watersheds. In urbanizing watersheds, it is critical that we understand how urbanization affects FDCs and stream flashiness. With an understanding of these interactions, we can better predict how urbanization will impact sediment yield metrics central to channel design.

In the second chapter of this paper, we aim to quantify the effects of urbanization on FDCs through a case study of streams spanning a gradient of urbanization in the Puget Sound region of Washington, USA. Using different time windows of the flow record, we quantify how key flow percentiles of the FDC changed with time in response to urbanization.

In the third chapter of this paper, we focus our efforts on quantifying the impact of flow data resolution on sediment yield metrics for streams of varying flashiness. In this analysis, we calculated the effective discharge, sediment yield, and half-load discharge using sediment rating curves over long time periods with both daily-averaged and sub-daily streamflow records to quantify the effects of flow data resolution on the calculation of sediment yield metrics for streams of varying flashiness.

1.1 REFERENCES

Ågren, A., Buffam, I., Jansson, M., & Laudon, H. (2007). Importance of seasonality and small streams for the landscape regulation of dissolved organic carbon export. *Journal of Geophysical Research: Biogeosciences*, 112(3).

Allan, J. D., & Castillo, M. M. (2007). *Stream Ecology: Structure and Function of Running Waters*. Springer Science & Business Media.

Booth, D. B. (1991). Urbanization and the natural drainage system--impacts, solutions, and prognoses. *Northwest Environmental Journal*, 7:93-118.

Boyd, M. J., Bufill, M. C., & Knee, R. M. (1993). Pervious and impervious runoff in urban catchments. *Hydrological Sciences Journal*, 38(6), 463-478.

Doyle, M. W., Shields, D., Boyd, K. F., Skidmore, P. B., & Dominick, D. (2007). Channel-forming discharge selection in river restoration design. *Journal of Hydraulic Engineering*, 133(7), 831-837.

Emmett, W. W., & Wolman, M. G. (2001). Effective discharge and gravel-bed rivers. *Earth Surface Processes and Landforms*, 26(13), 1369-1380.

Graf, W. L. (1977). Network characteristics in suburbanizing streams. *Water Resources Research*, 13(2), 459-463.

Hendon, S. (1995). Comparison of 15-Minute Versus Mean Daily Flow Duration Curves From The Yazoo Basin, MS. Masters Thesis, Colorado State University, Department of Civil and Environmental Engineering, Fort Collins, CO.

Hollis, G. E. (1975). The effect of urbanization on floods of different recurrence interval. *Water Resources Research*, 11(3), 431-435.

Leopold, L. B. (1968). *Hydrology for Urban Land Planning: A Guidebook on the Hydrologic Effects of Urban Land Use*. Washington, DC: US Geological Survey.

Price, K. (2011). Effects of watershed topography, soils, land use, and climate on baseflow hydrology in humid regions: A review. *Progress in physical geography*, 35(4), 465-492.

Putnam, A. L. (1972). *Effect of Urban Development on Floods in the Piedmont Province of North Carolina*. U.S. Geological Survey Open-File Report, 87 pp.

Simmons, D. L., & Reynolds, R. J. (1982). Effects of urbanization on base flow of selected south-shore streams, Long Island, New York. *Water Resources Bulletin,* 18:797-805.

Vogel, R. M., & Fennessey, N. M. (1994). Flow-duration curves. I: New interpretation and confidence intervals. *Journal of Water Resources Planning and Management*, 120(4), 485-504.

Vogel, R. M., Yaindl, C., & Walter, M. (2011). Nonstationarity: flood magnification and recurrence reduction factors in the United States. *Journal of the American Water Resources Association,* 47, 464-474.

Walling, D. E. (1977). Limitations of the rating curve technique for estimating suspended sediment loads, with particular reference to British rivers. *Erosion and solid matter transport in inland waters*, IAHS Publ. 122:34-48.

Walsh, C. J., Roy, A. H., Feminella, J. W., Cottingham, P. D., Groffman, P. M., & Morgan, R. P. (2005). The urban stream syndrome: current knowledge and the search for a cure. *Journal of the North American Benthological Society*, 24(3), 706-723.

2 CHAPTER 2: THE EFFECT OF URBANIZATION ON FLOW DURATION CURVES: A CASE STUDY FROM SELECTED STREAMS IN THE PUGET SOUND BASIN, WESTERN WASHINGTON

2.1 INTRODUCTION

World population has grown from 3.0 billion in the year 1960 to 6.1 billion in the year 2000, and is further expected to grow to 8.9 billion in the year 2050 (United Nations, 2004). With these tremendous increases in human population, many regions are devoting ever increasing land area to urban usage. Urban population centers are characterized by buildings, roads, sidewalks, and parking lots. These types of areas are traditionally impervious by nature, and therefore fundamentally alter hydrologic processes.

Urbanization is known to reduce the duration between the center of mass of rainfall excess and the peak flow rate, i.e, the lag time, of a watershed (Leopold, 1968). Lag time is reduced as water flows faster off of streets and roofs than naturally vegetated areas. Additionally, the advent of storm sewers and artificial drainage networks has contributed to the reduction of lag time in urban areas (Leopold, 1968). Impervious surfaces also reduce the amount of precipitation infiltrated; this combined with a shorter lag time often increases the peak magnitude of streamflow for a given precipitation event (Hollis, 1975).

Urbanization also causes fundamental changes in the sediment supply of rivers and streams. It has been suggested that during the construction phase of urbanization, sediment supply to the river increases, then as construction concludes; sediment supply to rivers may fall to very low levels (Wolman, 1967). In response to changes in water and sediment, rivers adjust their morphology (Schumm et al., 1984; Booth, 1990). Common forms of adjustment include changes in channel width, depth, and slope (Bledsoe and Watson, 2001). An understanding of

how river channels adjust their morphology to alterations in water and sediment supply caused by urbanization is critical to urban watershed planning and management.

Vogel et al. (2011) found that heavily urbanized locations had flood magnification factors ranging from 2-5, where a flood magnification factor is defined as a factor by which a past design flood quantile would have to be multiplied by to obtain the magnitude of the flood in the current time period. This work was done using annual maximum flood series, and therefore was focused on discharges greater than the 99^{th} percentile. This illustrates that urbanization generally results in large peak flows becoming more common. Urbanization has also been linked to the decline of stream baseflow in certain instances (Price, 2011; Simmons & Reynolds, 1982). This is generally thought to be the result of impervious surfaces limiting the infiltration of precipitation into the subsurface layers; however, declining baseflow can also be caused by shallow groundwater extractions (Sophocleous, 2002).

To represent the full spectrum of flows in a hydrologic record we often use a flow duration curve (FDC). A FDC is a graphic representation of the frequency and magnitude of all instantaneous, daily, weekly or monthly flows for a given period of time.

FDCs have a wide variety of applications in practice including water-use planning, flood control, and river and reservoir sedimentation (Vogel & Fennessey, 1994). They are also critical components of analytical channel design procedures that involve sediment transport such as the analysis of effective discharge (Wolman & Miller, 1960; Andrews, 1980) and the optimization of the sediment capacity-supply ratio (Biedenharn et al., 2000; Soar & Thorne, 2001). Because of the wide range of useful applications FDCs have, it is vital to understand how they respond to urbanization. Although there have been a number of studies focused on quantifying the effects of

urbanization on high- and low-magnitude discharges, its effects on the full spectrum of flows remains poorly understood.

In this paper, we present a case study on the effect of urbanization on FDCs for select streams in the Puget Sound Region of Western Washington using a 50-year analysis period starting in 1960 and ending in 2010. Objectives of the study include: (i) to tabulate urban growth in the selected watersheds; (ii) to evaluate precipitation trends; (iii) to quantify the effects of urbanization on FDCs and stream flashiness; (iv) to relate hydrologic changes to potential changes in channel morphology.

2.2 METHODS

2.2.1 STUDY AREA

The extent of this study is the Puget Sound basin of Western Washington, United States. This location was selected for this study because the Puget Sound basin has seen tremendous population growth in recent decades. The population of the four-county region of King, Kitsap, Pierce and Snohomish Counties has grown from approximately 1.5 million in 1960 to 3.7 million in 2010 (Washington State, 2012). In 2010, the Puget Sound basin comprised 70% of the state's population (Cuo et al., 2009).

The Puget Sound basin is bordered on the east by the Cascade mountain range and on the west by the Olympic Mountains. To the north, the basin extends towards Canada, with a small portion of the basin lying within British Columbia. To the south, the basin terminates in the foothills near the City of Olympia. The area of the basin is approximately 31,000 km^2 (Cuo et al., 2011). The region receives approximately 1000 mm of precipitation annually, with higher elevations receiving greater amounts. The majority of precipitation occurs as rain in the fall and

winter months, with over 75% of precipitation occurring between October and the end of March (Kruckeberg, 1991).

In the Puget lowlands, the dominant topographic features are deep generally north-south trending troughs (Collins et al., 2003). The features were formed by subglacial fluvial runoff from repeat advances of the Cordilleran ice sheet (Booth, 1994). Today, several of the region's large rivers pass through these wide, low gradient troughs (Collins et al., 2003). Most of the sediment deposits exposed at ground surface in the Puget lowland are products of glacial advance and retreat during the Vashon stade occurring 13,000-16,000 years ago (Booth et al., 2003). These sediments, known as Vashon Drift, include silt and clay, well-sorted sand and gravel, and unsorted sand and gravel (Booth et al., 2003).

2.2.2 SITE SELECTION

Because the effects of urbanization are most detectable in small watersheds, this analysis was limited to watersheds with a drainage area less than 200 km^2. To maintain a similar climate and precipitation amongst watersheds, only watersheds with a mean elevation less than 300 meters above sea level were included in this analysis. Lastly, selected watersheds were required to have at least 25 years of "adequate" discharge data collected at a United States Geological Survey (USGS) gaging station between 1960 and 2010. A year of flow record was considered "adequate" if more than half of the daily discharge observations were present. A map of the selected watersheds is shown in Figure 1. A table giving the drainage area, analysis period, and gage station number of each watershed is provided in Table 1.

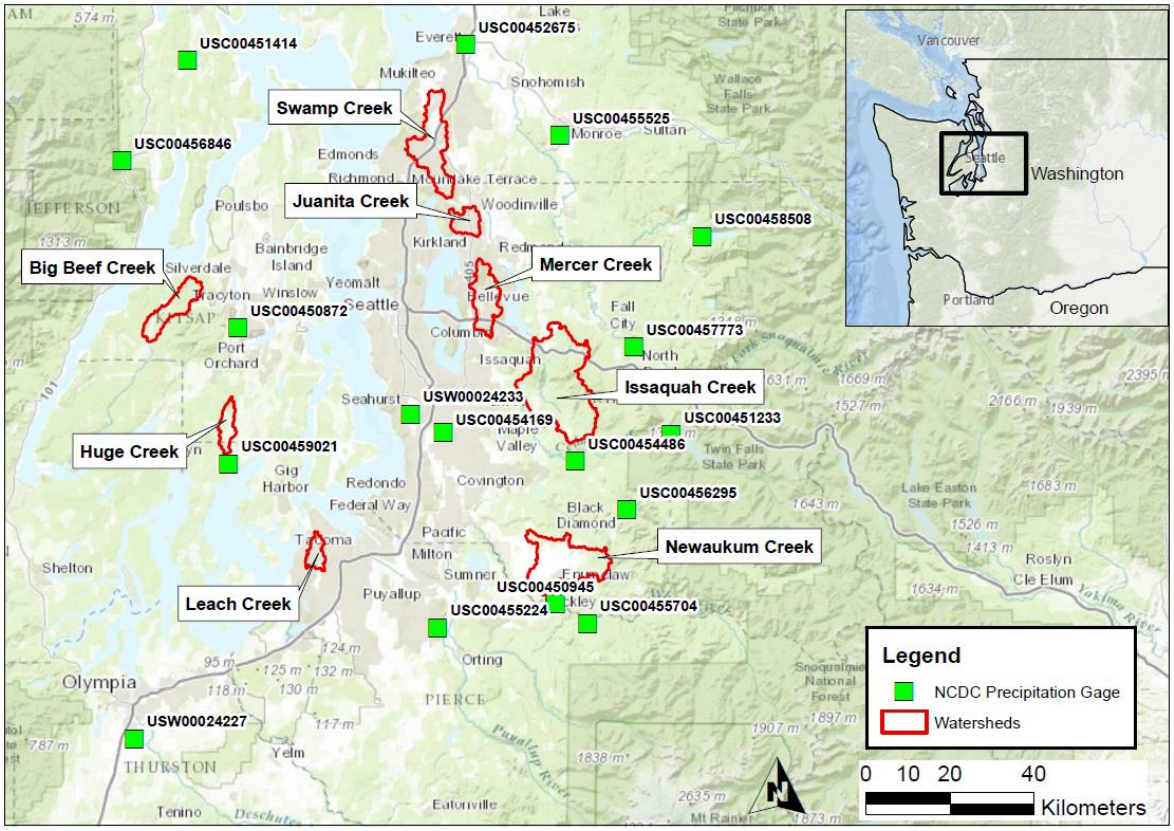

Figure 1: Map of watersheds and precipitation gages used in the analysis.

Table 1: Watersheds included in case study with associated analysis period, drainage area, and percent impervious cover.

Station Name	USGS Gage No.	Analysis Period	Drainage Area (km^2)	2011 Percent Impervious Surfaces
Juanita Creek near Kirkland, WA	12120500	1964-1989	17	40.9
Mercer Creek near Bellevue, WA	12120000	1960-2010	31	39.4
Swamp Creek at Kenmore WA	12127100	1964-1989	25	38.6
Big Beef Creek near Seabeck, WA	12069550	1970-1981, 1992-2007, 2009-2010	35	2.7
Huge Creek near Wauna, WA	12073500	1960-1969, 1978-2010	17	3.4
Newaukum Creek near Black Diamond, WA	12108500	1960-2010	70	7.0
Issaquah Creek near mouth near Issaquah, WA	12121600	1964-2010	145	6.4
Leach Creek near Fircrest, WA	12091200	1960-1986, 1989-2010	12.2	48.9

2.2.3 WATERSHED URBANIZATION ANALYSIS

The proportion of impervious surfaces in a watershed is an important indicator of urbanization. Increased streamflow rates and runoff volumes following urbanization are widely recognized to be caused by increases in impervious surface area (Boyd et al., 1993; Smith et al., 2002).

While watershed imperviousness is useful in quantifying urbanization, imperviousness datasets in the Puget Sound region are limited temporally. Satellite-derived estimates of impervious cover are available through the National Land Cover Dataset beginning in the year 2001 (Homer et al., 2004). However, because this study examines urbanization from 1960-2010, population density was chosen as the primary surrogate for urbanization. Strong relationships between watershed imperviousness and population density have been suggested in the literature (Stankowski 1972; Sheng & Wilson, 2009).

We used historic United States Census tract data to quantify population and population density in the watersheds over time. Geographic maps of census tract boundaries and associated population tables were obtained for censuses conducted in 1960, 1970, 1980, 1990, 2000, and 2010 (Minnesota Population Center, 2011). Census information is gathered in geographic units of varying size including: states, counties, tracts, and block levels. Census blocks offer population data at the finest spatial resolution but were not available for this region until the year 2000 (Minnesota Population Center, 2011). The finest-resolution population data available for the Puget Sound region from 1960-2010 were found to be census tract data. Therefore, census tract data were used to develop population estimates.

In order to examine the current relationship between impervious surfaces and population density in Washington State and to provide support for the use of population density as a surrogate for impervious cover, we compared population density in the year 2010 (Minnesota Population Center, 2011) against the average impervious percentage in the year 2011 (Homer et al., 2015) of each census tract in the state of Washington. In total, the relationship between population density and impervious cover was analyzed for more than 1200 census tracts.

Watershed populations for each decade were estimated from census tract data following the method of Sheng & Wilson (2009). Census tracts for each decade were re-mapped to the watershed boundaries in ArcGIS. For census tracts located only partially within the watershed, it was assumed that the census tract population density was uniform, and the population was split in proportion to the census tract area within the watershed. Population density (people/km^2) was then calculated by dividing the estimated watershed population (# of people) by the watershed area (km^2).

It should be noted that this method does not provide exact watershed populations because population densities in each census tract are not perfectly uniform. However, because urban census tracts are relatively small in area (often less than 10 km^2) we are confident that population densities are uniform enough to provide a reasonable estimate of watershed population on decadal time intervals.

2.2.4 PRECIPITATION

Daily precipitation series for each watershed from 1960-2010 were spatially interpolated from nearby National Climatic Data Center daily precipitation gages (Figure 1). An inverse distance weighting (IDW) procedure (Chen & Liu, 2012; Li & Heap, 2011; Lu & Wong, 2008)

was utilized. The equations used to perform the IDW procedure are provided below as Equations 1 and 2.

$$R_p = \sum_{i=1}^{N} w_i R_i \quad (1)$$

$$w_i = \frac{{d_i}^{-1}}{\sum_{i=1}^{N} {d_i}^{-1}} \quad (2)$$

In Equations 1 and 2, R_p is the unknown rainfall at the watershed of interest (mm); w_i is the weighting of rainfall station i; R_i is the rainfall at station i; d_i is the distance from rainfall station i to the centroid of the watershed of interest (km); lastly, N is the number of rainfall stations, which was the 5 nearest for this analysis (Appendix A).

Daily rainfall sequences were used to calculate a number of metrics aimed at quantifying different precipitation characteristics. To quantify the total magnitude of precipitation, the precipitation was summed on an annual basis. To capture the intensity of single and multiple day precipitation events, we calculated the maximum annual 1, 2, 3, and 7-day precipitation totals. Lastly, to quantify variability in precipitation we calculated the coefficient of variation of each year of daily precipitation records. The coefficient of variation is calculated by dividing the standard deviation of the distribution by the mean of the distribution.

2.2.5 FLOW METRICS

Temporal changes in streamflow were examined through analysis of the FDC. In order to track temporal changes in the FDC, a "cumulative-yearly" approach was taken. This means that a FDC was created for each year of the flow record using all years of record prior. To avoid any bias that may be introduced to the analysis by starting the analysis on an abnormally wet or dry year, the first cumulative FDC was created for the fifth year of record utilizing the first five years

of flow record. For each year after year five, a new FDC was created using the entire daily-averaged flow record to that given year. However, if a year had less than 50% of daily flow observations, it was excluded from the FDC analysis.

Another flow characteristic of interest to us in this analysis was the rate at which stream flow varies over time. Streams and rivers that experience rapid variations in streamflow over time are often termed "flashy." Watershed urbanization has been linked to flashy streamflow behavior in previous studies (Graf, 1977; Walsh et al., 2005). In this study we used the Richards-Baker Flashiness index (*RB*) (Baker et al., 2004) to characterize this behavior.

RB is calculated by first calculating the path length of flow changes over a given period of time. The path length is equal to the sum of the absolute values of day-to-day changes in discharge (q). This path length is then divided by the sum of mean daily flows (Equation 3).

$$RB = \frac{\sum_{i=1}^{n} |q_i - q_{i-1}|}{\sum_{i=1}^{n} q_i} \quad (3)$$

In Equation 3, i denotes the day and n is the number of days of flow record analyzed. The *RB* index is high for flashy hydrographs and low when hydrographs rise and fall gradually.

2.2.6 BASEFLOW ANALYSIS

Baseflow is a component of total streamflow that enters a stream from a persistent and slowly varying source (Sophocleous, 2002). While source of baseflow can vary, hydrologists agree that most baseflow originates from saturated flow from groundwater storage (Meyer, 2005). In order to examine trends in baseflow over the analysis period, the long-term hydrograph was separated into baseflow and runoff components. To isolate the baseflow in the long-term

hydrograph, the Web-based Hydrograph Analysis Tool (WHAT) was utilized (Lim et al., 2005). WHAT is not based on physical processes, but rather a statistical algorithm. For this study, a recursive digital filter method was used with filter parameters representative of "perennial streams with porous aquifers." When applied to hydrographs, this filter separates high-frequency signals associated with runoff from low-frequency signals associated with baseflow. Although the baseflow component of the hydrograph identified by this technique may not directly reflect groundwater contributions to streamflow, this methodology removes the subjective aspects from manual hydrograph separation and provides a fast and reproducible means to separating hydrographs over long periods of time (Lim et al., 2005).

Upon separation of the hydrograph into baseflow and direct runoff components, the average daily baseflow and direct runoff were computed for each year of record during the analysis period. Additionally, the baseflow index was calculated for each year of the analysis. The baseflow index, which is the long-term ratio of baseflow to total stream flow (Bloomfield et al., 2009), is useful for parametrizing streamflow by its origin.

2.2.7 STATISTICAL TESTS FOR TRENDS

The non-parametric Mann-Kendall test (Mann, 1945; Kendall, 1975) was used to identify statistically-significant trends in FDC percentiles, annual daily-average baseflow, annual daily-average runoff, and precipitation metrics. The Mann-Kendall test is designed to detect increasing or decreasing trends in data. The test is particularly useful as missing values are allowed and the data do not need to conform to any particular distribution (Gilbert, 1987). In this study, a *p*-value of 0.05 was used to identify significant trends.

2.2.8 ANALYSIS OF CHANNEL MORPHOLOGY

Two methods were used to relate hydrologic changes to potential changes in channel morphology. First, to relate changes in the FDC to changes in bed slope, Henderson proportionalities were used (Henderson, 1966). Henderson (1966) combined the Einstein sediment transport function as revised by Brown (1950), the Chezy flow resistance formula, and the conservation of momentum and mass for steady uniform flow into a single proportionality where q_s is the unit sediment transport rate, q is the unit water discharge, S is the channel slope, and D is the grain size (Equation 4).

$$q_s \propto \frac{q^2 S^2}{D^{\frac{3}{2}}} \tag{4}$$

Rearranging for channel slope yields:

$$S \propto \sqrt{\frac{D^{\frac{3}{2}} q_s}{q^2}} \tag{5}$$

The relationship in Equation 5 can be utilized to estimate the potential change in channel slope that would result from a given change in discharge. To do this, the channel slope at one point in time (S_1) is estimated from the unit sediment transport rate (q_{s1}) and unit discharge rate (q_1) at that same point in time. This can be done again at a second point in time to estimate the new channel slope (S_2).

$$\frac{S_1}{S_2} \propto \frac{\sqrt{\frac{q_{s_1}}{q^2{}_1}}}{\sqrt{\frac{q_{s_2}}{q^2{}_2}}} \tag{6}$$

Together S_1 and S_2 can be used to estimate the changes in slope that may result from shifts in the FDC induced by land use change over an analysis period as shown in Equation 6. For this study, unit sediment transport capacity was estimated at the 98th percentile discharge using a corrected version of the Meyer-Peter and Müller bedload transport equation (Wong & Parker, 2006). The bed material was considered gravel (Konrad et al., 2005), and held constant through time. Channel geometry as a function of depth was calculated using information from field measurements collected and made available by the USGS.

Secondly, hydraulic geometry relationships were utilized to relate changes in flow magnitude to potential changes in channel width. In an analysis of streams in the Puget Sound Lowland, many of which also appear in this study, Konrad et al., (2005) found that channel width (w) could be related to the 90th percentile discharge (Q_{90}) reasonably well through a power function:

$$w = 9.2Q_{90}^{0.39} \tag{7}$$

where w is in meters and Q_{90} is in m^3/s. To estimate the potential change in channel width resulting from urbanization-induced changes in flow, the Q_{90} was identified on a yearly basis from the cumulative flow record. Equation 7 was then used to establish an estimate of channel width on a yearly basis.

2.3 RESULTS

2.3.1 URBANIZATION ANALYSIS

Results of our analysis indicate that there is currently a strong relation between population density and impervious surfaces in the State of Washington. For census tracts with less than 50% impervious surface, as is the case with our eight study watersheds (Table 1),

population density was found to explain 74% of the variance in percent imperviousness (Figure 2). These results suggest that population density is a strong surrogate for impervious surfaces for watersheds that are less than 50% impervious.

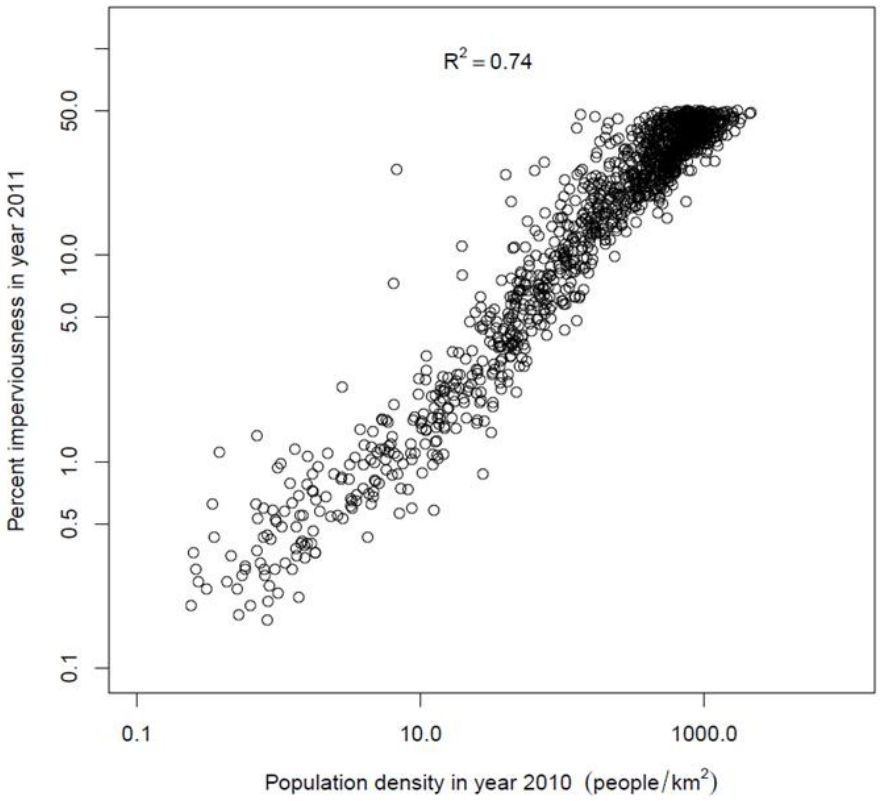

Figure 2: Relationship between impervious surfaces (computed from the 2011 NLCD, Homer et al., 2015) and population density for census tracts in the State of Washington that are less than 50% impervious.

Analysis of decadal populations in the watersheds revealed a wide range of population density (Figure 3). Huge Creek and Big Beef Creek, located west of Seattle in Kitsap County, were found to have the lowest population density over the analysis period. Newaukum Creek and Issaquah Creek were found to have slightly higher population densities, but both had slow growth rates similar to those in Huge and Big Beef Creeks. The remaining watersheds, Juanita,

Mercer, Swamp, and Leach Creeks, were found to have very large growth rates over the analysis period. Juanita Creek had the greatest population growth, growing from approximately 154 people/km^2 in 1960 to over 1900 people/km^2 in 2010. Mercer, Swamp, and Juanita Creeks all had similar growth trends to a lesser extent, growing from less than 300 people/km^2 in 1960 to more than 1500 people/km^2 in 2010. Leach Creek was already highly urbanized in 1960 and therefore saw lesser population growth over the analysis period.

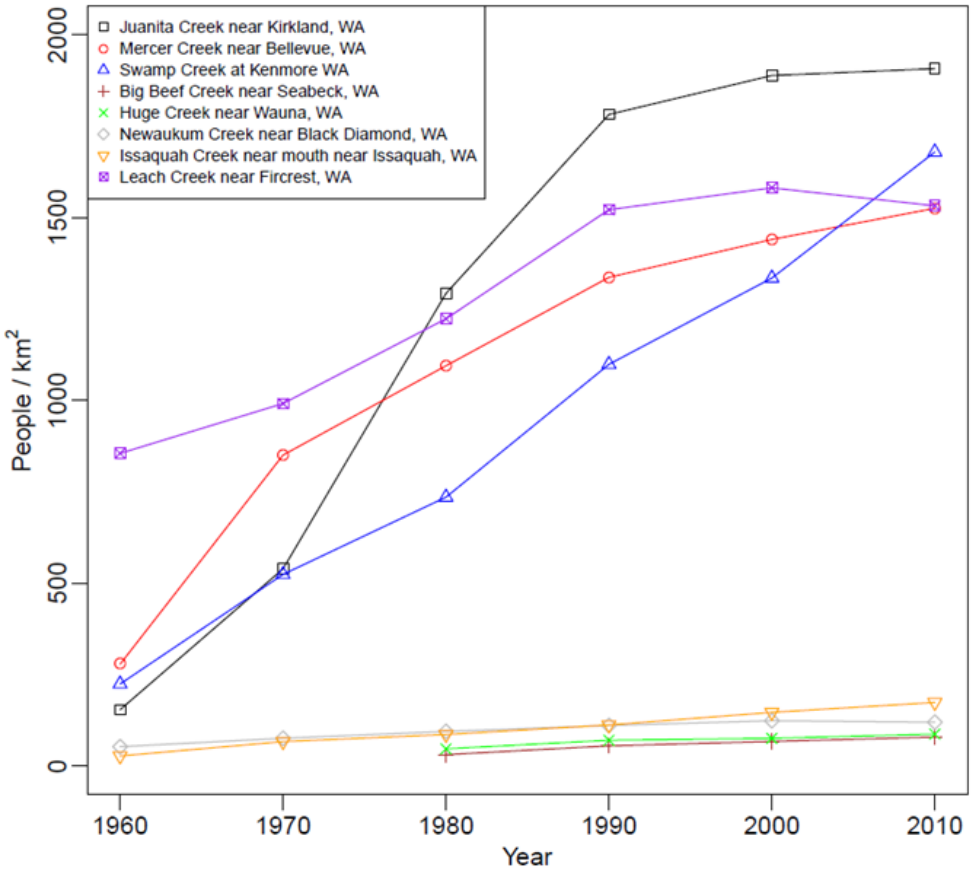

Figure 3: Estimation of watershed population density from 1960-2010 in the study watersheds.

Based on these results, the watersheds were categorized into two groups according to population density in 2010. Watersheds with a population density greater than 1,000 people/km^2 in 2010 were categorized as urban watersheds. Conversely, watersheds with a population density

of less than 1,000 people/km^2 in 2010 were categorized as rural watersheds. The results of this categorization are shown in Table 2.

Table 2: Categorization of study watersheds based on population density in the year 2010.

Station Name	USGS Gage No.	Estimated Population Density in 2010	Average Population Growth 1960-2010 (people/ km^2 / year)	Class
Juanita Creek near Kirkland, WA	12120500	1908	35.1	Urban
Mercer Creek near Bellevue, WA	12120000	1526	24.9	Urban
Swamp Creek at Kenmore WA	12127100	1680	29.1	Urban
Leach Creek near Fircrest, WA	12091200	1533	13.5	Urban
Newaukum Creek near Black Diamond, WA	12108500	120	1.3	Rural
Issaquah Creek near mouth near Issaquah, WA	12121600	174	2.9	Rural
Big Beef Creek near Seabeck, WA	12069550	79	1.6	Rural
Huge Creek near Wauna, WA	12073500	87	1.3	Rural

2.3.2 PRECIPITATION

Results of the precipitation analysis showed no statistically-significant trends in annual precipitation (Table 3). Two of the four urban watersheds (Mercer Creek and Leach Creek) and two of the four of the rural watersheds (Huge Creek and Big Beef Creek) were found to have statistically-significant increasing trends in multi-day precipitation maximums. All of the other watersheds showed slight but non-significant increases in multi-day precipitation maximums. Two of the eight watersheds (Leach Creek and Huge Creek) were found to have significant increasing trends in precipitation variability.

Table 3: Mann-Kendall tau values for precipitation metrics, a value of 1 indicates a perfect increasing trend while a value of -1 indicates a perfect decreasing trend.

			Mann-Kendall Tau Values Annual Maximum Precipitation				
Station Name	**Land Use**	**Annual Precipitation**	1-Day	2-Day	3-Day	7-Day	**Coefficient of Variation**
Juanita Creek near Kirkland, WA	Urban	-0.16 D	-0.04 D	0.02 U	0.08 U	0.06 U	-0.09 D
Mercer Creek near Bellevue, WA	Urban	-0.05 D	0.09 U	0.22 U**	0.20 U**	0.16 U**	0.00 -
Swamp Creek at Kenmore WA	Urban	-0.15 D	0.04 U	-0.04 D	0.08 U	0.14 U	-0.13 D
Leach Creek near Fircrest, WA	Urban	0.03 U	0.33 U**	0.32 U**	0.32 U**	0.26 U**	0.21 U**
Newaukum Creek near Black Diamond, WA	Rural	-0.11 D	0.05 U	0.11 U	0.02 U	0.03 U	-0.07 D
Issaquah Creek near mouth near Issaquah, WA	Rural	-0.07 D	0.15 U	0.08 U	0.06 U	0.02 U	0.11 U
Big Beef Creek near Seabeck, WA	Rural	-0.02 D	0.24 U**	0.21 U	0.25 U**	0.21 U	0.18 U
Huge Creek near Wauna, WA	Rural	0.01 U	0.31 U**	0.33 U**	0.38 U**	0.35 U**	0.27 U**

Notes: D= Downward Trend, U=Upward Trend

**Trend significant at p = 0.05 level

2.3.3 FLOW ANALYSIS

Three of the four urban watersheds had statistically-significant increasing trends over time in both the lower and higher portions of the FDC (Table 4). For high magnitude discharges (Q_{90}-Q_{99}), Leach Creek had the strongest increasing trend (Figure 4). Swamp Creek was the only urban watershed not to have an increasing trend in the upper portion of the FDC; however, it did have increases in the lower portion of the FDC. Combined, the urban watersheds experienced on average a 35% increase in the magnitude of the 98th (Q_{98}) and 99th (Q_{99}) percentile discharges (Table 5). The lower end of the FDC also increased in the urban watersheds but to a lesser degree (Table 5).

Three of the four rural watersheds had decreasing trends in the FDC. Newaukum Creek and Issaquah Creek had statistically-significant decreasing trends for all portions of the FDC. Huge Creek had statistically-significant decreasing trends for nearly all parts of the FDC except the 99th percentile discharge (Q_{99}), which had an increasing trend. The other rural watershed, Big Beef Creek, saw no statistically-significant trend with the exception of the 10th percentile discharge (Q_{10}). The magnitude of the decreasing trends for these watersheds was greatest in the lower part of the FDC. The 25th and 10th percentile flows decreased on average by 15% and 13%, while the 98th and 99th percentile flows decreased by only 2-3% on average (Table 5).

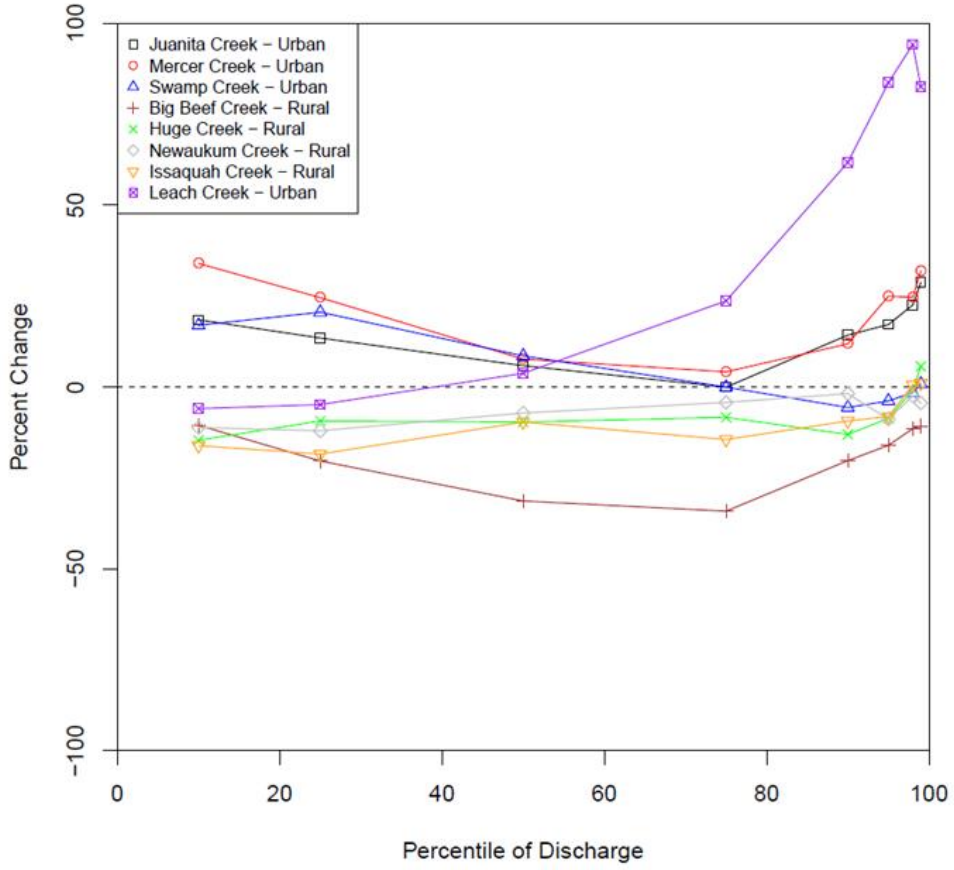

Figure 4: Percent change in FDC percentiles over the entire analysis period.

The urban watersheds were found to have much greater increases in the magnitude of the FDC than the rural watersheds. Leach Creek, an urban watershed, was found to have tremendous increases in the magnitude of 90^{th}-99^{th} percentile discharges (Figure 5a). In comparison, rural watersheds had slight decreases in the magnitude of the same discharges. Newaukum Creek, a rural watershed, was found to have a decreasing trend in the magnitude of 90^{th}-99^{th} percentile discharges (Figure 5b).

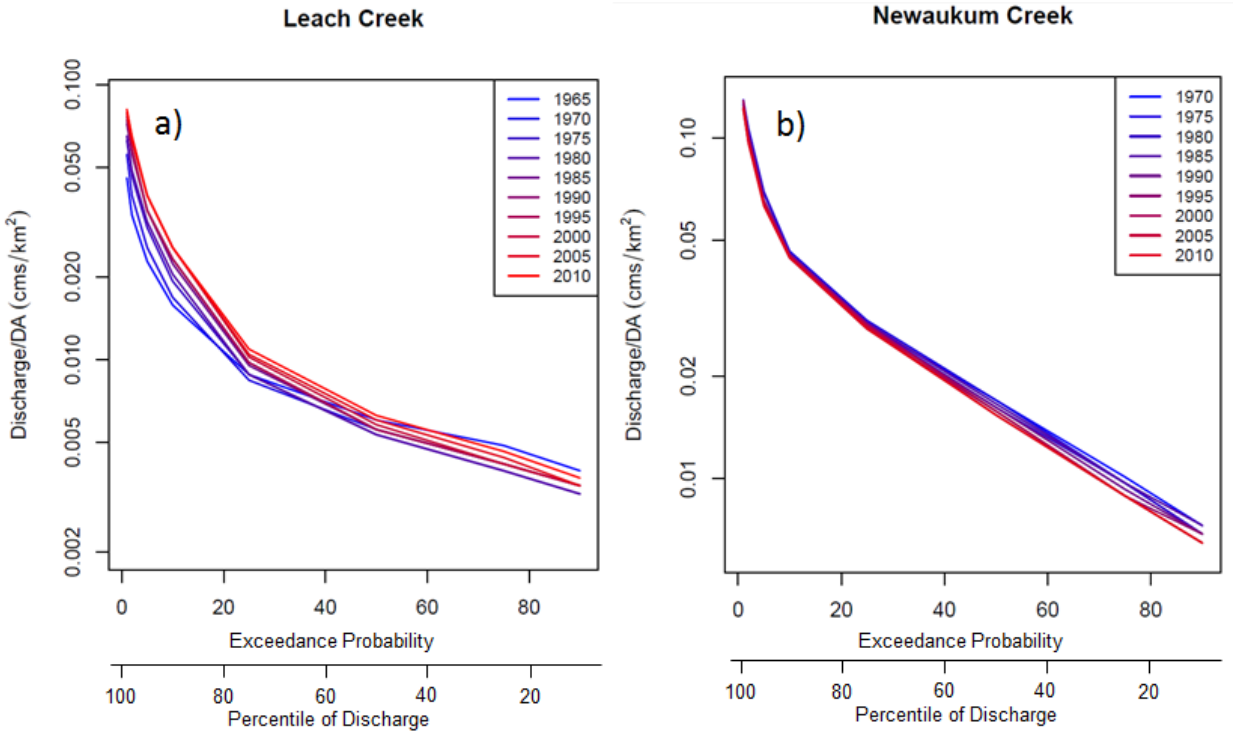

Figure 5: Temporal changes in the FDC of (a) Leach Creek (urban watershed) and (b) Newaukum Creek (rural watershed).

Results of our analysis on watershed flashiness yielded similar results across all watershed types. All watersheds with the exception of Newaukum Creek experienced statistically-significant increasing trends in Richards-Baker Flashiness (*RB*) over time (Table 4). The strongest increasing trends were generally found in the urban watersheds. Combined, the

average increase in flashiness for urban watersheds was 46% (Table 5). The rural watersheds saw flashiness increase on average by 9%.

Table 4: Mann-Kendall tau values for flow duration curve percentiles.

		Mann-Kendall Tau Values								
Station Name	**Land Use**	**Q_{10}**	**Q_{25}**	**Q_{50}**	**Q_{75}**	**Q_{90}**	**Q_{95}**	**Q_{98}**	**Q_{99}**	***RB***
Juanita Creek near Kirkland, WA	Urban	0.85 U**	0.82 U**	0.30 U	-0.11 D	0.56 U**	0.71 U**	0.75 U**	0.75 U**	1.00 U**
Mercer Creek near Bellevue, WA	Urban	0.47 U**	0.28 U**	-0.07 D	-0.16 D	0.1 U	0.63 U**	0.81 U**	0.85 U**	0.99 U**
Swamp Creek at Kenmore WA	Urban	0.87 U**	0.79 U**	0.56 U**	0.09 U	-0.47 D**	-0.48 D**	-0.44 D**	-0.35 D**	0.97 U**
Leach Creek near Fircrest, WA	Urban	0.38 U**	0.41 U**	0.47 U**	0.91 U**	0.92 U**	0.93 U**	0.95 U**	0.95 U**	0.74 U**
Newaukum Creek near Black Diamond, WA	Rural	-0.71 D**	-0.84 D**	-0.85 D**	-0.65 D**	-0.47 D**	-0.61 D**	-0.55 D**	-0.35 D**	0.13 U
Issaquah Creek near mouth near Issaquah, WA	Rural	-0.84 D**	-0.91 D**	-0.83 D	-0.85 D**	-0.76 D**	-0.77 D**	-0.51 D**	-0.32 D**	0.84 U**
Big Beef Creek near Seabeck, WA	Rural	-0.44 D**	-0.16 D	-0.1 D	-0.1 D	-0.29 D	-0.25 D	-0.23 D	-0.28 D	0.45 U**
Huge Creek near Wauna, WA	Rural	-0.81 D**	-0.66 D**	-0.61 D**	-0.47 D**	-0.52 D**	-0.26 D**	0.22 U	0.34 U**	0.67 U**

Notes: D= Downward Trend, U=Upward Trend

**Trend significant at p = 0.05 level

Table 5: Average percent change in flow metrics over analysis period.

	Average Percent Change %								
Land Use	**Q_{10}**	**Q_{25}**	**Q_{50}**	**Q_{75}**	**Q_{90}**	**Q_{95}**	**Q_{98}**	**Q_{99}**	***RB***
Urban	15.9	13.5	6.5	7.0	20.6	30.5	35.0	36.1	46.6
Rural	-13.1	-15.0	-14.4	-15.3	-11.1	-10.4	-3.5	-2.1	9.2

2.3.4 HYDROGRAPH ANALYSIS

Analysis of the baseflow and runoff components showed statistically-significant decreases in baseflow index for three of the four urban watersheds, Juanita Creek, Mercer Creek,

and Leach Creek (Table 6). A decrease in baseflow index can be caused by a decrease in baseflow, an increase in total streamflow, or both. In these three watersheds, the decrease in baseflow index was accompanied by a large increase in runoff, and subsequently an increase in total streamflow. Only one of these three watersheds, Mercer Creek, showed both an increase in runoff and a decrease in baseflow. Swamp Creek, the fourth urban watershed, saw a decreasing trend in baseflow index over the analysis, but the trend was not strong enough to be statistically significant. In total, the urban watersheds experienced a 43% increase in average daily runoff over the analysis period (Table 7).

Two of the four rural watersheds, Newaukum Creek and Issaquah Creek, were found to have statistically-significant downward trends in annual daily-average baseflow (Table 6). However, because of their decline in total streamflow, these watersheds did not have a statistically-significant decrease in baseflow index. No significant trends in baseflow, runoff, or baseflow index were found in the Huge Creek or Big Beef Creek. Overall, the rural watersheds had an average reduction in daily runoff of 6.8% and an average reduction in baseflow of 11.8% over the analysis period (Table 7).

Table 6: Mann-Kendall tau values for hydrograph analysis.

			Annual Daily-Average	
Station Name	**Land Use**	**Baseflow Index**	Runoff	Baseflow
Juanita Creek near Kirkland, WA	Urban	-0.55 D**	0.35 U**	-0.05 D
Mercer Creek near Bellevue, WA	Urban	-0.57 D**	0.25 U**	-0.19 D**
Swamp Creek at Kenmore, WA	Urban	-0.23 D	0.00 -	-0.19 D
Leach Creek near Fircrest, WA	Urban	-0.24 D**	0.46 U**	0.43 U**
Newaukum Creek near Black Diamond, WA	Rural	-0.10 D	-0.03 D	-0.17 D**
Issaquah Creek near mouth near Issaquah, WA	Rural	-0.07 D	-0.13 D	-0.26 D**
Big Beef Creek near Seabeck, WA	Rural	0.13 U	-0.05 D	-0.11 D
Huge Creek near Wauna, WA	Rural	-0.11 D	0.03 U	-0.09 D

Notes: D= Downward Trend, U=Upward Trend

**Trend significant at p = 0.05 level

Table 7: Average percent change in annual daily-average runoff and baseflow magnitude.

	Average % Change	
Land Use	**Runoff**	**Baseflow**
Urban	43.4	4.8
Rural	-6.8	-11.8

2.3.5 CHANNEL MORPHOLOGY

Using locally-calibrated bankfull geometry relationships (Konrad et al., 2005) and Henderson proportionalities (Henderson, 1966), we estimated the potential change in channel bankfull width and channel slope over the analysis period. Potential for change in channel slope and bankfull width were calculated independently of each other to provide end members of channel response. In reality, morphologic change in response to urbanization would likely include changes in both channel width and slope.

Findings from this analysis indicate the urban streams have significant potential for channel degradation. Over the analysis period, potential response of channel slope ranged from an 8.2% decrease to a 0.6% increase for urban watersheds. Potential channel bankfull width response ranged from a 2.2% reduction to a 20.6% increase (Table 8).

Table 8: Potential change in channel slope and width for urban and rural streams over the analysis period.

	Channel Slope		Channel Width	
Land Use	**Min.**	**Max.**	**Min.**	**Max.**
Urban	-8.2	0.6	-2.2	20.6
Rural	-0.3	4.5	-8.4	-0.7

Analysis of the rural streams indicates that the rural watersheds have potential for increases in channel slope (0 – 4.5%). However, channel width was predicted to decrease in these watersheds (0 – 8%). These results suggest overall potential for channel aggradation. Potential for change in channel morphology varies amongst urban and rural watersheds as hydrologic response to changes in land use also vary. Differences in geologic setting, stormwater infrastructure, and style of development all may contribute to this result.

2.4 DISCUSSION

2.4.1 IMPACT OF URBANIZATION ON THE FDC

Our results indicate that urbanization has the potential to significantly increase the magnitude of the entire FDC (Table 5). This result corresponds to other work showing that urbanization can cause significant increases in flood magnitude (Hejazi & Markus, 2009; Konrad, 2003). Increases in watershed imperviousness are known to cause increased streamflow rates and runoff volumes (Boyd et al., 1993; Smith et al., 2002); a result that is mirrored in this analysis.

While many studies have found that urbanization generally decreases the magnitude of low flows due to decreased contributions from groundwater storage (Price, 2011; Simmons & Reynolds, 1982; Rose & Peters, 2001), this study found that on average, the magnitude of low discharges (10^{th}-25^{th} percentile) increased in urban watersheds. This somewhat unexpected result is in part due to flow augmentation in one of the four urban watersheds. Since 1993, Leach Creek has had low flows augmented by a groundwater well (Kimbrough et al., 2001). It is not known if similar programs have been adopted at the other urban watersheds analyzed in this study. Others have suggested that increases in baseflow in urban watersheds can also be the result of leakages in storm sewer and water distribution systems, or lawn watering in certain regions (Meyer, 2002; Lerner, 2002). It is also possible that these results are influenced by an overestimation of baseflow resulting from using the WHAT baseflow separation method (Lim et al., 2005). The WHAT program uses a "local minimum method" that connects the local minimum points of the hydrograph by comparing slopes. This methodology may cause an overestimation of baseflow (and therefore an underestimation of runoff) during prolonged periods of rainy weather.

Results of the flow analysis for rural watersheds indicated that the magnitude of the extremely high discharges (98^{th}-99^{th} percentile) exhibited only a very slight decrease over time. Conversely, the magnitude of low discharges (10^{th}-25^{th} percentile) decreased substantially. Depending on the watershed, these decreases in magnitude were between 12-15% (Table 5). Big Beef Creek was the only rural watershed not to experience significant changes in flow magnitude. This result was likely caused by flow regulation from an upstream reservoir named Lake Symington (Kimbrough, 2001). We suspect that these results are to some degree the result of groundwater extraction. Groundwater is used in many of these watersheds for agricultural and municipal purposes. Demand on groundwater has reached such a high that in most watersheds,

nearly all of the groundwater is already legally allocated (Washington State Department of Ecology, 2012).

Groundwater extractions have been directly linked to reductions in streamflow in many locations (Winter, 1998). Additionally, strong evidence shows that groundwater and streamflow are highly interconnected in the Puget Sound basin (Morgan & Jones, 1999). Therefore, because of the high groundwater demand and usage in these watersheds, and the fact that groundwater extractions have been shown to reduce streamflow in this area, we believe that it is likely that groundwater extractions are contributing to the decreases in the magnitude of small streamflow discharges.

2.4.2 FLASHINESS

Flashiness was observed to increase greatly in our urban watersheds over the analysis period. This is likely largely due to the increase in impervious surfaces, and the advent of stormwater conveyance systems associated with urban development. This has been observed in previous studies across the country (Gregory & Calhoun, 2007; Schnoover et al., 2006) and within the Puget Sound Basin (Konrad & Booth, 2002). Urban growth and stream flashiness are plotted together in Figure 6 for Leach Creek. In Figure 6, we see stream flashiness increasing rapidly with population density from 1960-1990. From 1990-2010, population density begins to level out. During this same time, stream flashiness is also observed to approach a constant asymptotic value.

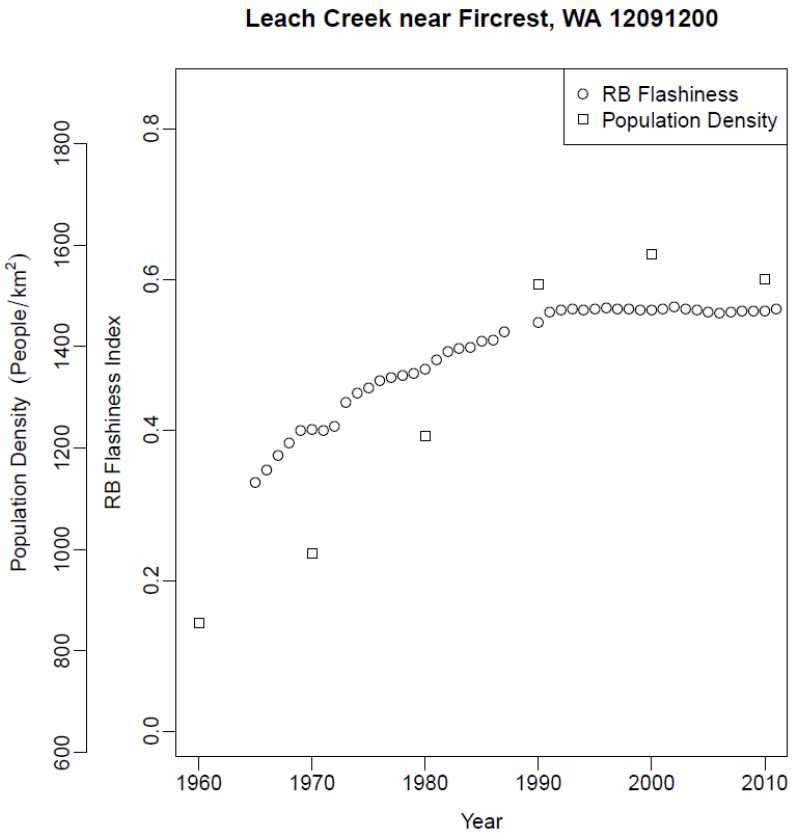

Figure 6: Temporal increases in stream flashiness and population density for Leach Creek.

In addition to changes in urbanization affecting flashiness, changes in precipitation may be impacting flashiness in two of the four urban watersheds (Leach Creek and Mercer Creek). Leach Creek was found to have significant increases in the magnitude of 1- to 7-day precipitation events and precipitation variation. Similarly, Mercer Creek was found to have significant increases in the magnitude of 2- to 7-day precipitation events.

In our rural watersheds, increases in stream flashiness are attributed to rural drainage improvements, and the increasing intensity and variability of precipitation in certain watersheds. Both of the rural watersheds had statistically-significant increases in the magnitude of annual 1-, 2-, 3- or 7-day maximum precipitation. Additionally, the variability of the precipitation was observed to increase for both rural watersheds. Lastly, reductions in baseflow contributed to

increases in *RB* stream flashiness in these regions by reducing the sum of the daily mean flows. These reductions cause the denominator of the *RB* flashiness metric to decrease, thereby causing the *RB* flashiness metric to increase.

This study demonstrated that while stream flashiness increases greatly in response to urbanization, flashiness may also increase in response to changing precipitation. This suggests that even watersheds with stationary land use may be becoming more flashy. Under increasing flashiness, daily-averaged data may poorly capture brief, high magnitude, sediment transporting discharges in flashy watersheds, thus underestimating sediment transport (see Chapter 3).

2.4.3 CHANNEL MORPHOLOGY

Hydrologic changes caused by urbanization have the potential to impact channel morphology (Hawley et al., 2012; Hammer, 1972). Increases in discharge caused by urbanization can cause channel degradation. Previous studies have linked urbanization to channel widening and incision (Booth, 1990; Galster et al., 2008). Additionally, stream flashiness can cause bank instability through rapid wetting and drawdown (Thorne, 1990). Through our study, we found that urban watersheds had the potential for channel degradation as a result of increasing flow magnitudes.

The method and magnitude by which a stream channel adjusts to increases in erosive force and stream power associated with urbanization is dependent, in part, on the stream's geologic setting. Streambanks with cohesive soils (Kang et al., 2006), dense riparian vegetation (Millar, 2000), or geologic controls (Nelson et al., 2006), may be resistant to increases in channel width. If the streambank exhibits greater resistance than the streambed, incision is a likely first response to increases in stream power associated with urbanization. Conversely, if the streambed

provides the greatest resistance, channel widening may be a first response. This highlights that the potential of morphologic change in response to urbanization is dependent on a number of factors including, geologic setting, vegetation, mode of sediment transport, and style and intensity of urbanization. In an analysis of two urbanizing streams in Washington State, Bledsoe & Watson (2001) found differences in the resistance of bed material, riparian vegetation, and the amount of time since development occurred, to be primary factors in the level of morphologic response observed in the channels.

In our analysis of the potential impacts of urbanization on channel morphology we evaluated the potential of channel widening and incision separately. However, it is often found that these processes are interconnected. Channel incision often creates bank instability which can lead to mass wasting of channel banks (Simon and Rinaldi, 2000). Furthermore, channel incision can migrate up and down channel networks causing bank instability and channel widening across great areas (Schumm et al., 1984). Our analysis did not account for interactions between adjustments in channel width and depth, or impacts of stream flashiness on channel widening. Additionally, because we did not account for the propagation of channel incision within a drainage network, it is likely that this analysis may be underestimating the potential morphologic impacts of urbanization.

In an examination of Bear and Soos Creek drainages in the Puget Sound basin of Washington, Booth (1990) found that a two-year discharge unit stream power of 80 watts/m^2, could be used as a predictor of bank erosion and channel incision. Unit stream power, ω, is calculated as shown in Equation 8 where ρ is the fluid density (kg/m^3), g is gravity (m/s^2), Q is stream discharge (m^3/s), S is slope (m/m), and w is channel width (m).

$$\omega = \frac{\rho g Q S}{w} \quad (8)$$

In our analysis, we have found that the unit stream power associated with the 2-year discharge has increased over the analysis period in our urban watersheds and is nearing the 80 watts/m^2 threshold described by Booth (Table 9). This result further indicates that channel incision may be a cause for concern in these watersheds.

Table 9: Increases in unit stream power of the 2-year discharge at urban watersheds.

Station Name	Land Use	Analysis		Unit Stream Power (W/m^2)	
		Begin	End	Begin	End
Juanita Creek near Kirkland, WA	Urban	1969	1989	45	63
Mercer Creek near Bellevue, WA	Urban	1965	2010	39	61
Swamp Creek at Kenmore, WA	Urban	1969	1990	62	72
Leach Creek near Fircrest, WA	Urban	1965	2010	26	35

While many studies have shown that urbanization increases the peak magnitude of flood events (Hejazi & Markus, 2009; Konrad, 2003), this study demonstrates that in certain regions, urbanization may increase the magnitudes of flows spanning the entire FDC. In these circumstances, the magnitude of high, median, and low flows all increase in response to urbanization. This result has important implications for sediment transport analyses such as the calculation of sediment yield and effective discharge. Additionally, increases in streamflow and sediment transport capacity affect channel morphology, often causing channel degradation in the form of channel widening or incision.

Channel widening and incision can cause large increases in the suspended sediment concentration of a river. High suspended sediment concentrations stress fish, impair spawning grounds (Newcombe & Macdonald, 1991), reduce light reaching photosynthetic organisms, and

disrupt macroinvertebrate lifecycles (Berry et al., 2003). Channel widening and incision can also damage vital infrastructure such as roads, culverts, and bridges. This reaffirms the critical importance of understanding urbanization's impacts on the FDC. A robust comprehension of urbanization's impacts on the FDC will help us avoid the detrimental consequences of channel instability.

2.5 CONCLUSIONS

In this study, our analysis of population trends showed that all watersheds experienced population growth over the analysis period of 1960-2010. Watersheds with the highest population density and growth were categorized as "urban" while the remaining watersheds were categorized as "rural". Analysis of precipitation trends from 1960-2010 revealed that none of the eight watersheds had significant increasing or decreasing trends in annual precipitation. The precipitation analysis did reveal, however, that half of the watersheds were experiencing increasing trends in the variability and intensity of precipitation.

Results of our case study on the effect of urbanization on flow duration curves for the Puget Sound region revealed that urbanization caused upward shifts in the magnitude of the entire flow duration curve for nearly all of the urban watersheds. This upward shift was greatest for the high magnitude flows (90^{th}-99^{th} percentile) and on average represented an increase of about 35% over the analysis period. The upward shift was lesser for the low magnitude flows (10^{th}-25^{th} percentile) and on average represented an increase of about 15% over the analysis period. Rural watersheds were found to have decreases in the magnitude of small discharges (10-25^{th} percentile). This result was attributed to a reduction in baseflow caused by groundwater extraction. Streamflow in nearly all the watersheds exhibited a significant trend of increasing

flashiness. Urban watersheds showed an average increase of 46% in *RB* over the analysis period while rural watersheds showed an average increase of 9%.

Hydrologic trends for both urban and non-urban watersheds were related to potential changes in channel morphology. Urban watersheds that saw upward shifts in the FDC were found to have potential for channel degradation over the analysis period. This degradation ranged from an 8.2% decrease to a 1.6% increase in channel slope. Urban watersheds were also found to have a potential for change in bankfull width ranging from a 2.2% reduction to a 20.6% increase. Conversely, rural watersheds, which saw a general downward shift in the FDC, were found to have potential for channel aggradation.

This study illustrates the dynamic influence of urbanization on hydrologic processes. Increasing precipitation intensity and variability, as well as anthropogenic changes in watershed land use, were found to impact streamflow magnitudes and frequencies over the analysis period. This illustrates the need for robust strategies for forecasting temporal shifts in the hydrologic record. Because FDCs are widely used by scientists and engineers for a wide range of applications including channel design and magnitude frequency analysis, future work that provides locally-calibrated estimates of FDC change with land use would be a valuable contribution to the field, and would advance hydrologic design procedures. Without an understanding of how FDCs change in response to urbanization, analytical channel design procedures such as the analysis of effective discharge will incur a greater degree of uncertainty and risk.

2.6 NOTATION

D = Grain size (mm)
d_i = Distance from rainfall station i to the centroid of the watershed of interest

g = Gravitational acceleration (m/s^2)
N = Number of rainfall stations
Q_x = x Percentile discharge (m^3/s)
Q = Discharge (m^3/s)
p = Probability of rejecting the null hypothesis when that hypothesis is true
ρ =Fluid density (kg/m^3)
q = Unit discharge (m^2/s)
q_i = Unit discharge on day i (m^2/s)
q_s = Unit sediment discharge (m^2/s)
R_i = Rainfall at station i (mm)
R_p = Unknown rainfall at watershed of interest (mm)
RB = Richards-Baker flashiness index
S = Channel bed slope (m/m)
W_i = Weighting of rainfall station i
w = Channel bankfull width (m)
ω = Unit stream power (W/m^2)

2.7 REFERENCES

Andrews, E. D. (1980). Effective and bankfull discharges of streams in the Yampa River basin, Colorado and Wyoming. *Journal of Hydrology*, 46(3), 311-330.

Baker, D. B., Richards, R. P., Loftus, T. T., & Kramer, J. W. (2004). A new flashiness index: characteristics and applications to Midwestern rivers and streams. *Journal of the American Water Resources Association*, 40(2), 503-522.

Berry, W., Rubinstein, N., Melzian, B., & Hill, B. (2003). The biological effects of suspended and bedded sediment (SABS) in aquatic systems: a review. *United States Environmental Protection Agency Internal Report; 102*.

Biedenharn, D. S., Copeland, R. R., Thorne, C. R., Soar, P. J., Hey, R. D., and Watson, C. C. 2000. "Effective discharge calculation: A practical guide." Technical Rep. No. ERDC/CHL TR-00-15, U.S. Army Corps of Engineers, Washington, D.C.

Bledsoe, B. P., & Watson, C. C. (2001). Effects of urbanization on channel instability. *Journal of the American Water Resources Association,* 37:255-70/

Bloomfield, J. P., Allen, D. J., & Griffiths, K. J. (2009). Examining geological controls on baseflow index (BFI) using regression analysis: An illustration from the Thames Basin, UK. *Journal of Hydrology*, 373(1), 164-176.

Booth, D. B. (1990). Stream channel incision following drainage-basin urbanization. *Journal of the American Water Resources Association,* 26(3), 407-417.

Booth, D. B. (1994). Glaciofluvial infilling and scour of the Puget Lowland, Washington, during ice-sheet glaciation. *Geology*, *22*(8), 695-698.

Booth, D.B., Haugerund, R.A., Goetz Troost, K. (2003). The Geology of Puget Lowland Rivers. In *Restoration of Puget Sound Rivers* (pp 14-46). Seattle, WA: University of Washington Press.

Boyd, M. J., Bufill, M. C., & Knee, R. M. (1993). Pervious and impervious runoff in urban catchments. *Hydrological Sciences Journal*, 38(6), 463-478.

Brown, C. B. (1950). Sediment transportation. In *Engineering hydraulics*, ed. H. Rouse. New York: Wiley. pp. 769-857.

Chen, F. W., & Liu, C. W. (2012). Estimation of the spatial rainfall distribution using inverse distance weighting (IDW) in the middle of Taiwan. *Paddy and Water Environment*, 10(3), 209-222.

Collins, B.D., Montgomery, D.R., Sheikh, A.J. (2003). Reconstructing the Historical Riverine Landscape of the Puget Lowland. In *Restoration of Puget Sound Rivers* (pp 79-129). Seattle, WA: University of Washington Press.

Cuo, L., Beyene, T. K., Voisin, N., Su, F., Lettenmaier, D. P., Alberti, M., & Richey, J. E. (2011). Effects of mid-twenty-first century climate and land cover change on the hydrology of the Puget Sound basin, Washington. *Hydrological Processes*, 25(11), 1729-1753.

Cuo, L., Lettenmaier, D. P., Alberti, M., & Richey, J. E. (2009). Effects of a century of land cover and climate change on the hydrology of the Puget Sound basin. *Hydrological Processes*, 23(6), 907-933.

Department of Ecology State of Washington. (2012). Focus on Water Availability: Kitsap Watershed WRIA 15 (Publication No. 11-11-020). Retrieved from https://fortress.wa.gov/ecy/publications/publications/1111020.pdf.

Department of Ecology State of Washington. (2012). Focus on Water Availability: Duwamish-Green Watershed, WRIA 09 (Publication No. 11-11-014). Retrieved from https://fortress.wa.gov/ecy/publications/publications/1111014.pdf.

Galster, J. C., Pazzaglia, F. J., & Germanoski, D. (2008). Measuring the Impact of Urbanization on Channel Widths Using Historic Aerial Photographs and Modern Surveys. *Journal of the American Water Resources Association*, 44(4), 948-960.

Gilbert, R.O., (1987). *Statistical methods for environmental pollution monitoring*. New York: John Wiley & Sons.

Graf, W. L. (1977). Network characteristics in suburbanizing streams. *Water Resources Research*, 13(2), 459-463.

Gregory MB, Calhoun DL (2007). Physical, chemical, and biological responses of streams to increasing watershed urbanization in the Piedmont Ecoregion of Georgia and Alabama, Chapter B of Effects of urbanization on stream ecosystems in six metropolitan areas of the United States. *U.S. Geological Survey Scientific Investigations Report 2006–5101-B.* Available from http://pubs.usgs.gov/sir/2006/5101B.

Hammer, T. R. (1972). Stream channel enlargement due to urbanization. *Water Resources Research*, 8(6), 1530-1540.

Hawley, R. J., Bledsoe, B. P., Stein, E. D., & Haines, B. E. (2012). Channel evolution model of semiarid stream response to urban-induced hydromodification. *Journal of the American Water Resources Association*, 48(4), 722-744.

Hejazi, M. I., & Markus, M. (2009). Impacts of urbanization and climate variability on floods in Northeastern Illinois. *Journal of Hydrologic Engineering*, 14(6), 606-616.

Henderson, F. M. (1966). *Open Channel Flow*. New York: MacMillan Publishing.

Hollis, G. E. (1975). The effect of urbanization on floods of different recurrence interval. *Water Resources Research*, 11(3), 431-435.

Homer, C., Huang, C., Yang, L., Wylie, B., & Coan, M. (2004). Development of a 2001 national Land-Cover Database for the United States. *Photogrammetric Engineering & Remote Sensing*, 70(7), 829−840.

Homer, C.G., Dewitz, J.A., Yang, L., Jin, S., Danielson, P., Xian, G., Coulston, J., Herold, N.D., Wickham, J.D., and Megown, K., 2015, Completion of the 2011 National Land Cover Database for the conterminous United States-Representing a decade of land cover change information. *Photogrammetric Engineering and Remote Sensing*, v. 81, no. 5, p. 345-354

Kang, R. S., & Marston, R. A. (2006). Geomorphic effects of rural-to-urban land use conversion on three streams in the Central Redbed Plains of Oklahoma. *Geomorphology*, *79*(3), 488-506.

Kendall, M.G., (1975). *Rank Correlation Methods*, 4th ed. Charles Griffin, London.

Kimbrough, R.A., Smith, R.R., Rupert, G.P., Wiggins, W.D., Knowles, S.M., and Renslow, V.F. (2001). *Water Resources Data, Washington, Water Year 2000*: U.S. Geological Survey Water-Data Report WA-00-1, 541p.

Konrad, C. P. 2003. Effects of urban development on floods. United States Geological Survey Fact Sheet 076–03, Tacoma, Washington.

Konrad, C. P., & Booth, D. B. (2002). *Hydrologic trends associated with urban development for selected streams in the Puget Sound Basin, western Washington*. United States Geological Survey Water-Resources Investigations Report 02–4040, Tacoma, Washington.

Konrad, C. P., Booth, D. B., & Burges, S. J. (2005). Effects of urban development in the Puget Lowland, Washington, on interannual streamflow patterns: consequences for channel form and streambed disturbance. *Water Resources Research*, 41(7).

Kruckeberg, A. R. (1991). *The natural history of Puget Sound country*. University of Washington Press.

Leopold, L. B. (1968). *Hydrology for Urban Land Planning: A Guidebook on the Hydrologic Effects of Urban Land Use*. Washington, DC: US Geological Survey.

Lerner, D. N. (2002). Identifying and quantifying urban recharge: a review. *Hydrogeology Journal*, 10(1), 143-152.

Li, J., & Heap, A. D. (2011). A review of comparative studies of spatial interpolation methods in environmental sciences: performance and impact factors. *Ecological Informatics*, 6(3), 228-241.

Lim, K. J., Engel, B. A., Tang, Z., Choi, J., Kim, K. S., Muthukrishnan, S., & Tripathy, D. (2005). Automated web GIS based hydrograph analysis tool, WHAT. *Journal of the American Water Resources Association*, 41, 1407-1416.

Lu, G. Y., & Wong, D. W. (2008). An adaptive inverse-distance weighting spatial interpolation technique. *Computers & Geosciences*, 34(9), 1044-1055.

Mann, H.B., 1945. Non-Parametric tests against trend, *Econometricia* 13:245-249.

Meyer, S. C. (2005). Analysis of base flow trends in urban streams, northeastern Illinois, USA. *Hydrogeology Journal*, 13(5-6), 871-885.

Meyer. S.C., 2002. Investigation of Impacts of Urbanization on Base Flow and Recharge Rates, Northeastern Illinois: Summary of Year 2 Activities. In: *Proceedings of 12th Annual Research Conference: Research on Agricultural Chemicals and Groundwater Resources in Illinois.*

Millar, R. G. (2000). Influence of bank vegetation on alluvial channel patterns. *Water Resources Research*, *36*(4), 1109-1118.

Minnesota Population Center. *National Historical Geographic Information System: Version 2.0*. Minneapolis, MN: University of Minnesota 2011.

Morgan, D. S., & Jones, J. L. (1999). Numerical model analysis of the effects of ground-water withdrawals on discharge to streams and springs in small basins typical of the Puget Sound Lowland, Washington. *U.S. Geological Survey Water Supply Paper*, (2492), 1-73.

Nelson, P. A., Smith, J. A., & Miller, A. J. (2006). Evolution of channel morphology and hydrologic response in an urbanizing drainage basin. *Earth Surface Processes and Landforms, 31*(9), 1063-1079.

Newcombe, C. P., & MacDonald, D. D. (1991). Effects of suspended sediments on aquatic ecosystems. *North American Journal of Fisheries Management*, 11(1), 72-82.

Price, K. (2011). Effects of watershed topography, soils, land use, and climate on baseflow hydrology in humid regions: A review. *Progress in physical geography*, 35(4), 465-492.

Rose, S., & Peters, N. E. (2001). Effects of urbanization on streamflow in the Atlanta area (Georgia, USA): a comparative hydrological approach. *Hydrological Processes*, 15(8), 1441-1457.

Schoonover, J. E., Lockaby, B. G., & Helms, B. S. (2006). Impacts of land cover on stream hydrology in the west Georgia piedmont, USA. *Journal of Environmental Quality,* 35(6), 2123-2131.

Schumm, S. A., Harvey, M. D., & Watson, C. C. (1984). Incised channels: morphology, dynamics, and control. Water Resources Publications. Littleton, CO. 208p.

Sheng, J., & Wilson, J. P. (2009). Watershed urbanization and changing flood behavior across the Los Angeles metropolitan region. *Natural Hazards*, 48(1), 41-57.

Simmons, D. L., & Reynolds, R. J. (1982). Effects of urbanization on base flow of selected south-shore streams, Long Island, New York. *Water Resources Bulletin,* 18:797-805.

Simon, A. & Rinaldi, M. (2000). Channel instability in the Loess area of the Midwestern United States. *Journal of the American Water Resources Association*, 36(1), 133-150.

Smith, J. A., Baeck, M. L., Morrison, J. E., Sturdevant-Rees, P., Turner-Gillespie, D. F., & Bates, P. D. (2002). The regional hydrology of extreme floods in an urbanizing drainage basin. *Journal of Hydrometeorology*, 3(3), 267-282.

Soar, P. J., and Thorne, C. R. (2001). Channel restoration design for meandering rivers. *Rep. No. ERDC/CHL CR-01-1*, U.S. Army Engineer Research and Development Center, Vicksburg, Miss.

Sophocleous, M. (2002). Interactions between groundwater and surface water: the state of the science. *Hydrogeology Journal*, 10(1), 52-67.

Stankowski, S. J. (1972). Population density as an indirect indicator of urban and suburban land-surface modifications. *U.S. Geological Survey Professional Paper, 800-B*, B219-B224.

Thorne, C. R. 1990. Effects of vegetation on riverbank erosion and stability. Pages 125–144 in J. B. Thornes (ed.), *Vegetation and erosion: processes and environments*. Wiley and Sons, New York.

United Nations, Department of Economic and Social Affairs. 2004. *World Population to 2300.* United Nations, NY.

Vogel, R. M., & Fennessey, N. M. (1994). Flow-duration curves. I: New interpretation and confidence intervals. *Journal of Water Resources Planning and Management*, 120(4), 485-504.

Vogel, R. M., Yaindl, C., & Walter, M. (2011). Nonstationarity: flood magnification and recurrence reduction factors in the United States. *Journal of the American Water Resources Association*, 47, 464-474.

Walsh, C. J., Roy, A. H., Feminella, J. W., Cottingham, P. D., Groffman, P. M., & Morgan, R. P. (2005). The urban stream syndrome: current knowledge and the search for a cure. *Journal of the North American Benthological Society*, 24(3), 706-723.

Washington State (2012). Historical Data Set: Decennial Population Counts for the State, Counties, Cities and Towns: Office of Financial Management. Available at: http://www.ofm.wa.gov/pop/april1/hseries/default.asp

Winter TC, Harvey JW, Franke OL, Alley WM (1998). Ground water and surface water – a single resource. U.S. Geological Survey Circular 1139:79.

Wolman MG, Miller JP. (1960). Magnitude and frequency of forces in geomorphic processes. *Journal of Geology*, 68:54-74.

Wong, M., & Parker, G. (2006). Reanalysis and correction of bed-load relation of Meyer-Peter and Müller using their own database. *Journal of Hydraulic Engineering*, 132(11), 1159-1168.

3 CHAPTER 3: THE EFFECT OF FLOW DATA RESOLUTION ON SEDIMENT YIELD ESTIMATION AND CHANNEL DESIGN

3.1 INTRODUCTION

Reliable streamflow records at appropriate resolutions are vital for a variety of scientific and engineering applications. In the United States, the United States Geological Survey (USGS) operates more than 7,000 streamflow gages (Olson & Norris, 2007). At these gages, river stage is usually measured every 15 to 60 minutes and converted to a discharge using a rating curve (Olson & Norris, 2007). These data are then made freely available online in either daily-averaged or sub-daily (usually 15-min) time steps.

Streamflow records are used for a variety of purposes including flood frequency analysis (Vogel et al., 2011), sediment yield calculations (Wheatcroft & Sommerfield, 2005), and natural channel design (Skidmore et al., 2001). Daily-averaged discharges are often used in conjunction with sediment rating curves to obtain an estimate of sediment transport rate and sediment yield (Milliman & Meade, 1983; Simon, 1989; Syvitski & Morehead, 1999), which can be important criteria for dominant discharge determination and channel design (Doyle et al., 2007). Sediment rating curves are an empirical best-fit power function relating streamflow and sediment discharge (Walling, 1977). By using daily-averaged discharge data in these types of calculations, one must assume that this type of data does an adequate job of representing the flow regime. However, studies have shown that small (Ågren et al., 2007), urban (Graf, 1977; Walsh et al., 2005), and arid watersheds (Allan & Castillo, 2007) can exhibit rapid short-term variations in streamflow during runoff events. This type of streamflow behavior is termed “flashy.” In flashy watersheds, high sediment transporting discharges may happen infrequently and for very brief periods of time; in these situations, daily-averaged flow data may not adequately capture the flows most important for sediment transport.

It was recognized long ago that using sediment rating curves with daily-averaged flow data could cause errors in the computation of sediment discharge if the daily-average discharge is not representative of the flow rate throughout the day (Colby, 1956). Because sediment discharge is non-linearly related to stream discharge, small errors in the magnitude of streamflow may cause large errors in the estimation of sediment transport. A study of six watersheds in East Devon, England showed that sediment yield calculations from daily flow records could vary by up to 10% from those made with instantaneous records (Walling, 1977). However, it is not clear how flashiness was related to the error in sediment yield calculations for these watersheds.

A study of small to medium-size watersheds (smaller than 620 km^2) of the Yazoo River basin in Northwest Mississippi revealed that sediment yield curves created from daily-averaged flow data can deviate from 15-minute sediment yield curves by more than 100% (Hendon, 1995). This was because the highest discharges, occurring less than 3% of the time, were not represented in the daily-averaged data. Missing these discharges is problematic because high discharge rates correspond to high sediment transport rates. In another study from the same basin, use of daily-average flow data was found to under predict sand yield by 51% and total suspended sediment yield by 59% (Dubler, 1997). While these studies provide insight, they do not explain how these results are related to stream flashiness.

To the best of our knowledge, the effect of flow data resolution on sediment transport calculations has not been investigated outside of the Yazoo River Basin and East Devon, England or with a large set of sites. Additionally, while the aforementioned studies investigated the effect of flow data resolution on sediment yield calculations, the relationship with flashiness remains unquantified. We hypothesize that errors in sediment transport and yield calculations based on daily-average flow data systematically increase with stream flashiness.

In this paper, we present our findings from a study of the effect of flow data resolution on sediment transport metrics for both bedload and suspended load transport for rivers across the United States. The objectives of this paper are threefold: (i) to quantify the effect of flow data resolution (daily-averaged and sub-daily) on sediment yield calculations in light of stream flashiness; (ii) to identify the situations in which using daily-averaged flow data for sediment transport calculations is acceptable and when it is not; (iii) to investigate the potential impacts on channel design parameters when daily-averaged flows are used in situations where sub-daily flows are more appropriate.

3.2 METHODS

3.2.1 DATA SELECTION

This analysis drew from bedload and suspended load sites that were assembled for another study focused on magnitude-frequency analysis of U.S. streams and rivers (Sholtes, 2015). Sites were analyzed individually for continuity in flow records and effects of flow regulation. In total, 39 sites with bedload measurements and 99 sites with suspended load measurements were chosen to be included in this analysis (Figure 7). All bedload and suspended load measurements were taken from published articles and government reports as the original source of all sediment transport data (Sholtes, 2015). In these articles and reports, bedload transport was measured with Helley-Smith samplers, and suspended sediment was measured using standard USGS techniques. The sites cover a wide range of the conterminous United States and represent drainage areas ranging from approximately 10 to 2,500,000 km^2 (Appendix B). Basins were chosen such that a wide range of flow regime types would be analyzed including flashy and non-flashy systems.

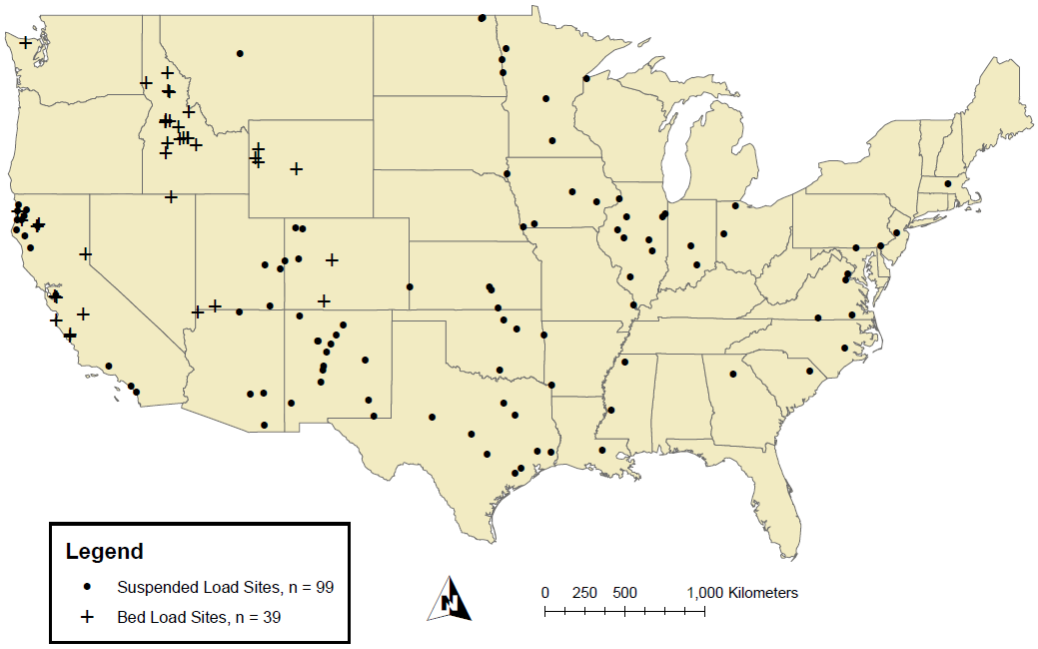

Figure 7: Map of sites used in this study.

Daily flow data and sub-daily flow data (after Oct. 1, 2007) were downloaded from USGS National Water Information System Website (NWIS). Sub-daily flow data (prior to Oct. 1, 2007) were obtained through the USGS Instantaneous Data Archive (IDA). The record length of flow data retrieved varied by site but ranged from the first day in which sub-daily flow data were available through the water year 2013, if possible. Some gages were discontinued prior to 2013; in that case, data were retrieved through the date in which the gage ceased operations. In total, 80 percent of sites used in this analysis contained more than 10 years of flow data.

3.2.2 DATA FILTERING

Flow data downloaded from the USGS were filtered prior to analysis. All blank observations and observations of "ice" were removed. Additionally, due to lapses in both the daily and sub-daily flow data, the flow data had to be filtered so that time series of both datasets were identical. For example, if the month of September 1995 was missing from the sub-daily flow data,

the month of September 1995 was removed from the daily-averaged data, and vice-versa. Additionally, because sub-daily flow data prior to Oct. 1, 2007 are stored by the USGS in the IDA, while data after this date are accessible from the NWIS, the sub-daily flow data had to be combined to create a seamless time series. For some sites, the sub-daily flow data were a mix of 15-min observations and observations on the hour. To ensure consistent flow data resolution for our analysis, all sub-daily flow data were sampled on the top of the hour to create a consistent set of hourly observations.

3.2.3 FLASHINESS

Because it was hypothesized that sub-daily flow data would be most useful for flashy systems for which daily-averaged flow data do not adequately represent the flow regime, stream flashiness was calculated with daily-averaged flow data at each site. Several methods have been proposed for quantifying stream flashiness (Baker et al., 2004; Konrad & Booth, 2002); here we use the Richards-Baker flashiness index (Baker et al., 2004).

The Richards-Baker flashiness index (*RB*) is calculated by first calculating the path length of flow changes over a given period of time. The path length is equal to the sum of the absolute values of day-to-day changes in discharge. This path length is then divided by the sum of mean daily flows. The *RB* index is high for flashy hydrographs and low when hydrographs rise and fall gradually. The *RB* index is shown below in Equation 9 where q is the daily-averaged discharge, i is the day, and n is the total number of days in the flow record.

$$RB\ Index = \frac{\sum_{i=1}^{n} |q_i - q_{i-1}|}{\sum_{i=1}^{n} q_i} \quad (9)$$

3.2.4 SEDIMENT RATING CURVES

In order to characterize the rate at which sediment is transported as a function of flow, sediment rating curves were employed. Sediment rating curves often take the form of a simple power function: $Q_s = aQ^b$, where Q_s is the sediment discharge rate, Q is the water discharge rate, and a and b are best fit regression parameters (Asselman, 2000). In this relationship, it has been suggested that the exponent *b* is related to the transport capacity in excess of sediment supply, while the coefficient *a* is related to absolute sediment supply (Barry et al., 2007).

The sediment rating curves used in this study were obtained from Sholtes (2015) where the source data and process of developing these curves are explained in detail. For the sake of brevity, the process is only briefly described in this paper. Each site included more than 15 sediment discharge measurements, and a sufficiently long flow record spanning the time in which the sediment data were collected. For suspended load sites, the fraction of sediment ≥ 0.0625 mm in diameter (sand) was isolated and used as it best approximates dominant bed material. Using these data, rating curves were developed that relate measured sediment transport to discharge using a log-linear or power-law relationship. A quality-control procedure was used to cull sites with poor rating curve fits (e.g., $R^2 < 0.50$) or sparse data. The rating curves are of the form: $Q_s = a * BCF * Q^b$, where Q_s is the sediment discharge rate (kg/s), a is a best fit coefficient, *BCF* is a logarithmic bias correction factor, Q is the water discharge $\left(\frac{m^3}{s}\right)$, and b is the best fit exponent. When creating a sediment rating curve, it is often necessary to apply a logarithmic bias correction factor (BCF) to avoid systematic bias introduced by the logarithmic transformation (Ferguson, 1987). For more information on the regression procedures used to create the sediment rating curves see Sholtes (2015).

3.2.5 SEDIMENT TRANSPORT METRICS

In order to characterize sediment discharge at each site, three sediment transport metrics were calculated using both the daily averaged and the sub-daily flow data. The three sediment transport metrics utilized in this study are the effective discharge (Q_{Eff}), the discharge below which 50% of the sediment is transported (Q_{s50}), and the sediment yield (SY).

The term effective discharge refers to the increment of discharge that transports the largest fraction of the annual sediment load over a period of years (Andrews, 1980). For some streams and rivers, the effective discharge is often considered to be the "channel forming discharge" and nearly equivalent to bankfull discharge (Andrews, 1980). The effective discharge is generally computed by first subdividing the range of streamflows observed during a period of record into a number of classes or bins from which the total sediment quantity transported by each class is calculated. This is achieved by multiplying the frequency of flow occurrence in each class by the median sediment load for that flow class (Biedenharn et al., 2000), resulting in a sediment yield. The sediment load for a flow was calculated using a sediment rating curve. The effective discharge (Q_{Eff}) is the median discharge of the flow class with the maximum sediment yield. This concept is depicted in Figure 8.

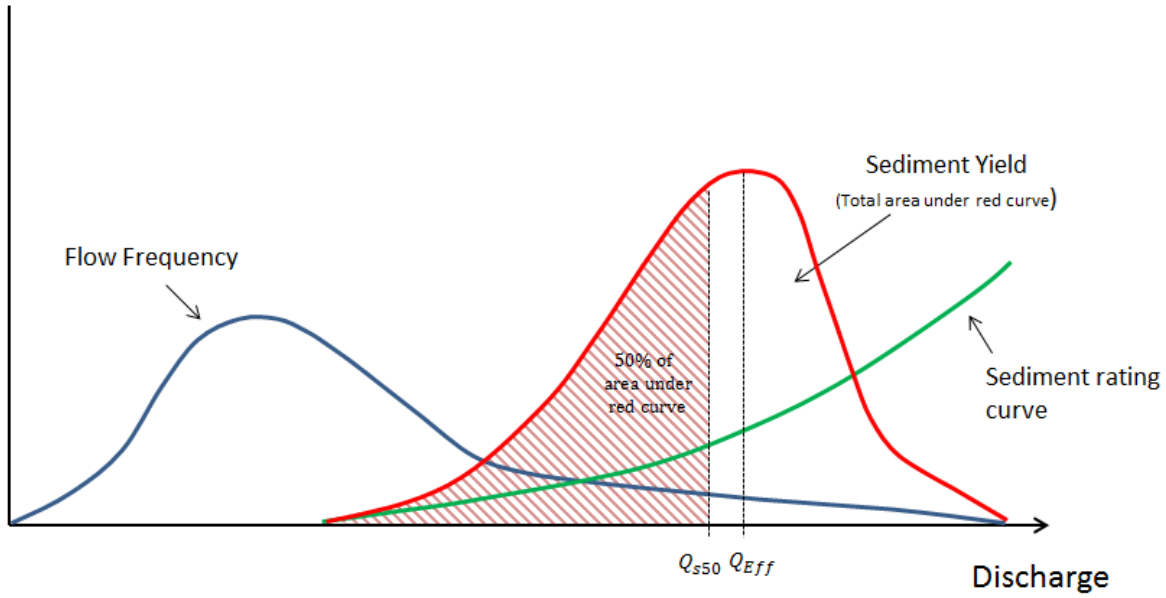

Figure 8: Qualitative illustration of sediment transport metrics used in this study.

To compute the effective discharge using actual flow records, the discharge data are typically discretized into a histogram. The bins of the histogram can be spaced either arithmetically or logarithmically. For this study, effective discharge was calculated using an arithmetic binning procedure. Effective discharge has been calculated by others using both arithmetic and logarithmic bins, however, the majority of analyses have chosen arithmetic bins (Soar & Thorne, 2001). Initially 25 arithmetic bins were used in the analysis based on the literature (Biedenharn et al., 2000); however, if the effective discharge fell into the first bin, the first bin was subdivided into three new bins and the analysis was repeated. This was done to prevent the under-estimation of effective discharge. If the effective discharge fell into the first bin again, the original first bin was subdivided into 5 bins. This process was repeated until the effective discharge no longer occurred in the first bin or until the original first bin has been subdivided into 11 or more bins. Once the bin with the maximum sediment yield was identified, the median flow in that bin was deemed the effective discharge.

The sediment rating curve and streamflow frequency histogram were multiplied to create a sediment yield curve. By performing a trapezoidal integration (trapz function, PRACMA package, R CORE Team, 2014) procedure on the sediment yield curve (red line, Figure 8), the total sediment yield for the multi-year period of record was obtained. Sediment yield is graphically depicted as the area under the red line in Figure 8.

Lastly, to calculate the half-load discharge (Q_{s50}), an ordered vector of sediment discharges was created by sorting the water discharges and applying the sediment rating curve. The ordered sediment discharge vector was then cumulatively summed. Q_{s50} was then determined by locating the water discharge that corresponded to 50% of the cumulative sediment transport, Q_{s50}, which can be greater than or less than Q_{Eff} depending on the shape of the sediment yield curve, is graphically depicted in Figure 8.

3.2.6 RESPONSE VARIABLES

In order to investigate the effect of flow data resolution on Q_{Eff}, SY, and Q_{s50}, we divided the sediment transport metrics computed from daily-averaged flow data by those which were computed with sub-daily flow data. The resulting ratios (SY_{Daily} / SY_{Sub}, $Q_{Eff\text{-}Daily}$ / $Q_{Eff\text{-}Sub}$, $Q_{s50\text{-}Daily}$ / $Q_{s50\text{-}Sub}$) indicate the degree of dissimilarity in the results.

3.2.7 QUANTILE REGRESSION

Quantile regression (Koenker & Bassett, 1978) was used to analyze the relationships between our response variables (SY_{Daily} / SY_{Sub}, $Q_{Eff\text{-}Daily}$ / $Q_{Eff\text{-}Sub}$, $Q_{s50\text{-}Daily}$ / $Q_{s50\text{-}Sub}$) and flashiness. While most regression applications estimate rates of change in the mean of the response variable, quantile regression estimates rates of change for all portions of a probability distribution of the response variable (Cade & Noon, 2003). Quantile regression is especially useful for regression models with heterogeneous variances. In these circumstances, ordinary

regression techniques may underestimate, overestimate, or fail to identify real changes in the heterogeneous distribution (Cade & Noon, 2003).

3.2.8 MULTIPLE LINEAR REGRESSION

Multi-variable linear regression was utilized to model relationships between response and predictor variables. A database of site characteristics and flow metrics was analyzed to identify the best subsets (regsubsets function, LEAPS package, R CORE Team, 2014) of predictor variables. The database of predictor variables included bed sediment size data (Sholtes, 2015), annual precipitation derived from 30-year normals (PRISM Group, 2015), drainage areas, and flow metrics derived from USGS streamflow records. Predictor variables identified in each best subset were checked for cross-correlation before being regressed. A maximum R^2 value of 0.20 was allowed amongst variables in a regression model. Best subsets of 1 and 2 variables were identified. Use of an interaction variable (the product of two variables) was also explored. A regression model that utilizes an interaction variable may take the generic form of Equation 10.

$$\frac{SY_{Daily}}{SY_{Sub}} = C_1 + C_2X + C_3Y + C_4XY \quad (10)$$

In Equation 10, *X* and *Y* are variables used to predict the ratio of sediment yield computed with daily-averaged flow data (SY_{Daily}) to the sediment yield computed with sub-daily flow data (SY_{Sub}). In this equation, C_1, C_2, C_3, and C_4 are constants and *XY* is the interaction variable.

3.3 RESULTS

3.3.1 EFFECTIVE DISCHARGE

Flashiness did not impact the ratio of effective discharge computed with daily-averaged flow data ($Q_{Eff\text{-}Daily}$) to effective discharge computed with sub-daily flow data ($Q_{Eff\text{-}Sub}$) (Figure

9). Of the bedload sites, approximately 60% had a $Q_{Eff\text{-}Daily}$ / $Q_{Eff\text{-}Sub}$ ratio that was larger than one. Similarly, of the suspended load sites, 40% had a $Q_{Eff\text{-}Daily}$ / $Q_{Eff\text{-}Sub}$ ratio that was larger than one. It was observed that for flashy (RB > 0.3) bedload sites, the ratio of $Q_{Eff\text{-}Daily}$ / $Q_{Eff\text{-}Sub}$ tended to be greater than 1. Flashiness also appeared to be related to error in $Q_{Eff\text{-}Daily}$ for suspended load sites. As RB flashiness increases, the departure of $Q_{Eff\text{-}Daily}$ / $Q_{Eff\text{-}Sub}$ from 1 was observed to increase.

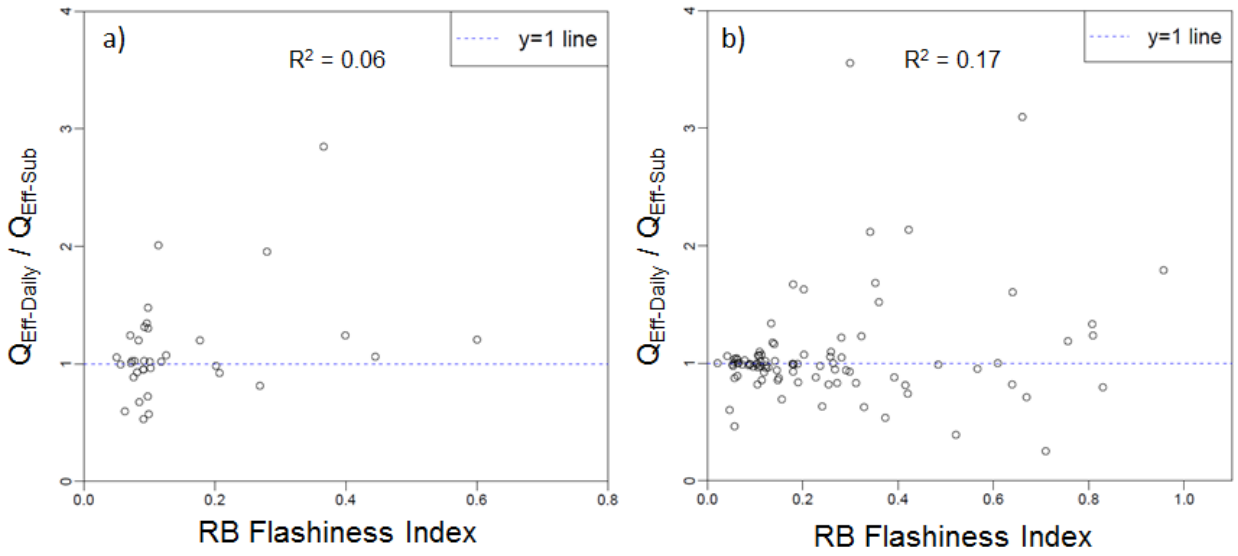

Figure 9: Ratio of effective discharge computed with daily-averaged flow to sub-daily flow vs. the Richards-Baker flashiness index: a) bedload sites b) suspended load sites.

3.3.2 QUANTILE REGRESSION

3.3.2.1 Sediment Yield

Sediment yield computed with daily-averaged flow data (SY_{Daily}) was found to generally be less than sediment yield computed with sub-daily flow (SY_{Sub}) (Figure 10). The ratio of SY_{Daily} / SY_{Sub} was found to decrease with flashiness in a wedge-shaped fashion for both bedload and suspended load sites. That is, for non-flashy sites ($RB \approx 0.1$), SY_{Daily} / SY_{Sub} was found to be nearly equal to 1 while for flashy sites (RB > 0.4), SY_{Daily} / SY_{Sub} was found to range from 1 to

0.4. Quantile regression was used to highlight the heterogeneous response of SY_{Daily} / SY_{Sub} to flashiness. In Figure 10, the various "quantile" lines represent different parts of the response variable distribution. In this case, we used quantile regression to highlight the 5th, 25th, 50th, 75th, and 99th percentiles of the SY_{Daily} / SY_{Sub} distribution to flashiness (Figure 10). It was also observed that the sediment rating curve parameter *b* contributed to the degree of response of SY_{Daily} / SY_{Sub} to flashiness: for sites with flashy flow characteristics, as *b* increases, the ratio of SY_{Daily} / SY_{Sub} decreases (Figure 11).

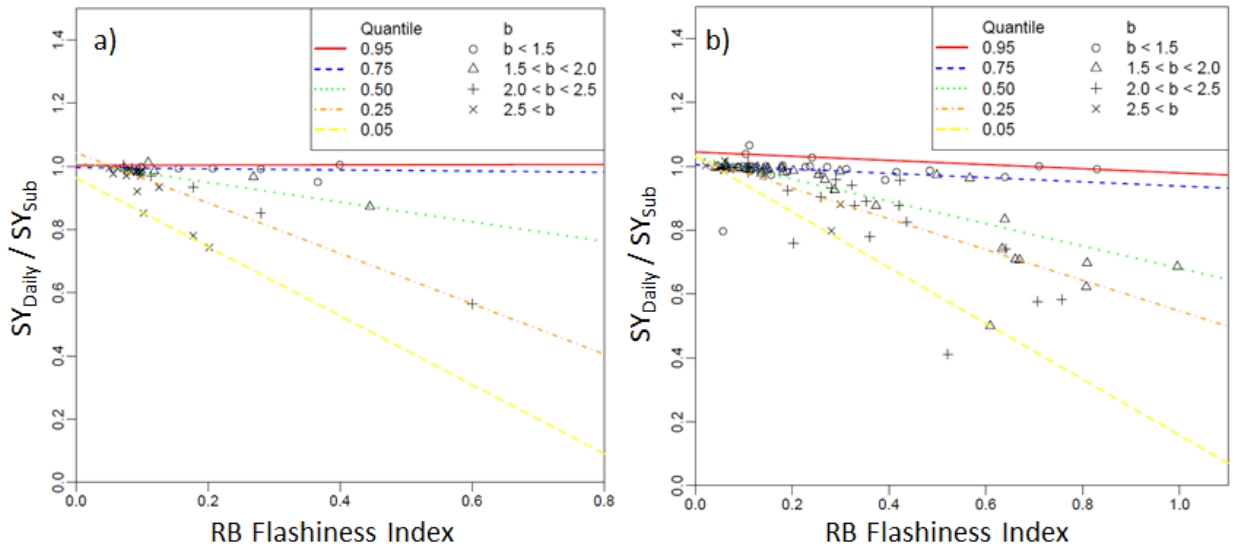

Figure 10: Ratio of sediment yield computed with daily-averaged flow to sub-daily flow vs. the Richards-Baker flashiness index: a) bedload sites b) suspended load sites.

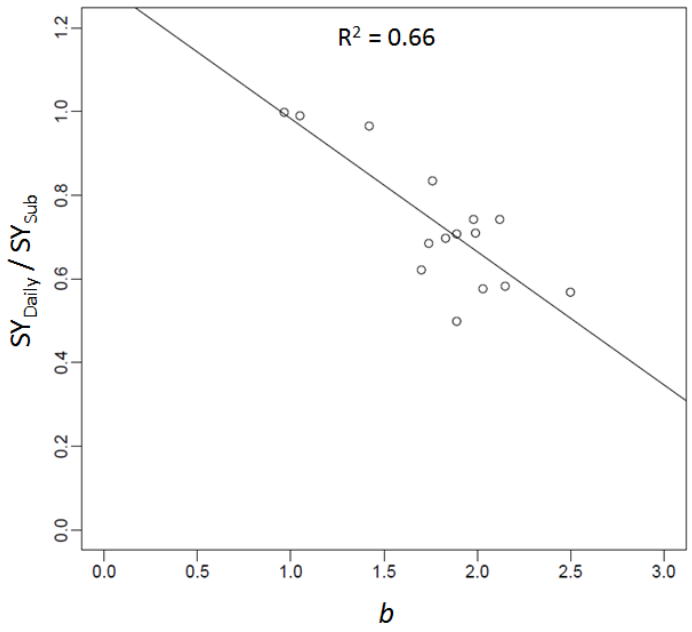

Figure 11: Relationship between the underestimation of sediment yield and the sediment rating curve best fit exponent, *b*, for suspended load sites with a *RB* flashiness greater than 0.6.

3.3.2.2 Half –load discharge (Q_{s50})

The half-load discharge calculated with daily flow data ($Q_{s50\text{-}Daily}$) was found to generally be less than when it was calculated with sub-daily flow data ($Q_{s50\text{-}Sub}$) (Figure 12). Much like the *SY* data, the Q_{s50} data formed a wedge-shaped pattern in which the sediment rating curve parameter *b* influenced the degree of response of $Q_{s50\text{-}Daily}$ / $Q_{s50\text{-}Sub}$. That is, for non-flashy sites (RB ≈ 0.1), $Q_{s50\text{-}Daily}$ / $Q_{s50\text{-}Sub}$ was found to be nearly equal to 1, while for flashy sites (RB > 0.4), $Q_{s50\text{-}Daily}$ / $Q_{s50\text{-}Sub}$ was found to range from 1 to 0.2. The sediment rating curve parameter *b* also contributed to the degree of response of $Q_{s50\text{-}Daily}$ / $Q_{s50\text{-}Sub}$ to flashiness. For sites with flashy flow characteristics, as rating curve parameter *b* increased, the ratio of $Q_{s50\text{-}Daily}$ / $Q_{s50\text{-}Sub}$ decreased.

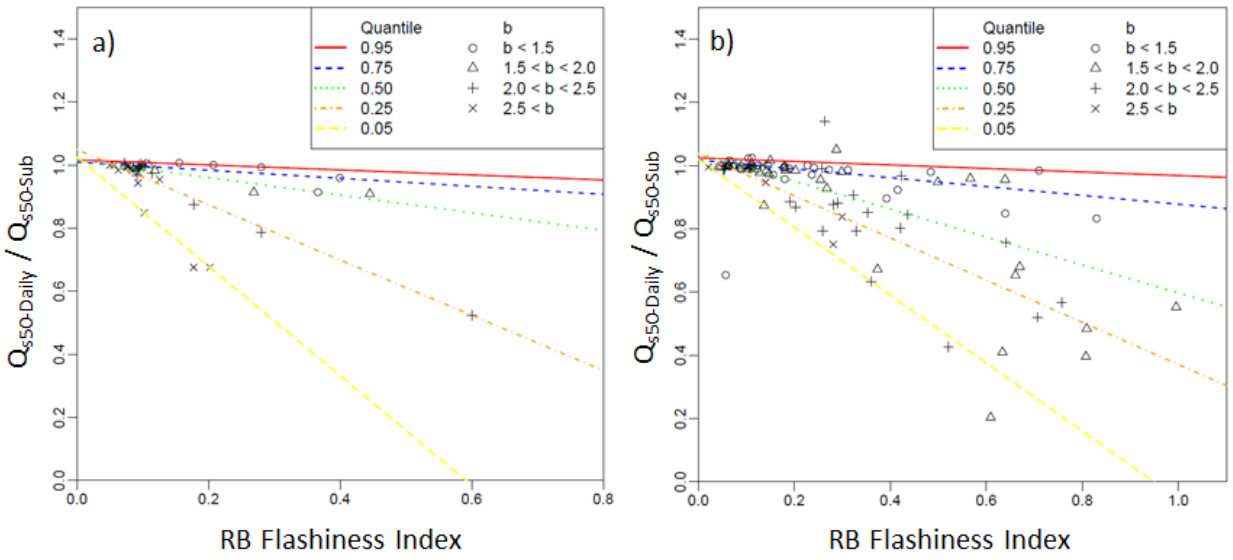

Figure 12: Ratio of discharge below which 50% of sediment is transported computed with daily-averaged flow to sub-daily flow vs. the Richards-Baker flashiness index: a) bedload sites b) suspended load sites

3.3.3 MULTIPLE LINEAR REGRESSION ANALYSIS

The best predictors of change in SY_{Daily} / SY_{Sub} and $Q_{s50\text{-}Daily}$ / $Q_{s50\text{-}Sub}$ were identified through multiple linear regression analysis (Table 10). Variables used in the analysis include *RB*, average annual precipitation, drainage area, median bed sediment size (d_{50}), 84th-percentile bed sediment size (d_{84}), best-fit sediment rating curve exponent (b), and best-fit sediment rating curve coefficient (a). *RB* was found to be the best single predictor of change in both in SY_{Daily} / SY_{Sub} and $Q_{s50\text{-}Daily}$ / $Q_{s50\text{-}Sub}$ for both bedload and suspended load sites as it explained more variance than any other single variable (i.e., higher R^2 value). The second- and third-best indicators for all models were b and d_{50}. Explanatory power increased from a 1-variable model to a 2-variable model. The best model, based on adjusted R^2, was found to be a 2-variable interaction model that utilized *RB* and b. All models in Table 10 are significant at $p < 0.0001$.

Table 10: Linear regression models for the prediction of SY_{Daily} / SY_{15} *and* $Q_{s50\text{-}Daily} / Q_{s50\text{-}15}$ for suspended and bedload sites.

Bedload / Suspended Load	Dependent Variable	Number of regression model parameters	Best Regression Model	Adj. R^2
Bedload	SY_{Daily} / SY_{15}	1	1.0184 - 0.4472 RB	0.371
Bedload	SY_{Daily} / SY_{15}	2	1.1123 - 0.5514 RB - 0.0293 b	0.507
Bedload	SY_{Daily} / SY_{15}	2 + interaction	0.95 + 0.6297 RB + 0.03937 b - 0.5715 RB*b	0.824
Bedload	$Q_{s50\text{-}Daily} / Q_{s50\text{-}15}$	1	1.0279 - 0.5511 RB	0.380
Bedload	$Q_{s50\text{-}Daily} / Q_{s50\text{-}15}$	2	1.117 - 0.6518 RB - 0.02834 beta	0.459
Bedload	$Q_{s50\text{-}Daily} / Q_{s50\text{-}15}$	2 + interaction	0.9393 + 0.6569 RB + 0.0478 beta - 0.633 RB*beta	0.718
Suspended Load	SY_{Daily} / SY_{15}	1	1.053 - 0.407 RB	0.330
Suspended Load	SY_{Daily} / SY_{15}	2	1.1802 - 0.4085 RB - 0.06994 b	0.374
Suspended Load	SY_{Daily} / SY_{15}	2 + interaction	1.0126 + 0.3832 RB + 0.02115 b - 0.4300 RB*b	0.456
Suspended Load	$Q_{s50\text{-}Daily} / Q_{s50\text{-}15}$	1	1.04 - 0.50 RB	0.476
Suspended Load	$Q_{s50\text{-}Daily} / Q_{s50\text{-}15}$	2	1.118 – 0.50 RB – 0.04265 b	0.490
Suspended Load	$Q_{s50\text{-}Daily} / Q_{s50\text{-}15}$	2 + interaction	0.9917 + 0.09672 RB + 0.02573 beta - 0.3246 RB*beta	0.532

RB = Richards-Baker Flashiness index computed with daily-average flow data
b = Best fit exponent from sediment rating curve

d50 = median grain size (mm)

3.4 DISCUSSION

3.4.1 EFFECTIVE DISCHARGE

The decision to use daily-averaged or sub-daily streamflow data was not found to impact the calculation of effective discharge in a consistent way. Amongst bedload and suspended load sites, the ratio of $Q_{Eff\text{-}Daily} / Q_{Eff\text{-}Sub}$ was both less than 1 and greater than 1 in nearly equal abundance. We believe that these results are a byproduct of the inherently variable process of determining Q_{Eff}.

Upon further inspection it was found that for ratios of $Q_{Eff\text{-}Daily} / Q_{Eff\text{-}Sub}$ less than unity, differences in the size of the bins (range of discharges) in the discretized flow duration curve histogram were the primary cause for the differences in Q_{Eff}. We refer to this as a Type A error.

Type A errors were caused by the sub-daily flow record nearly always has a larger maximum flow and smaller minimum flow than the daily-averaged flow record. This greater range between the maximum and minimum flow forces the range of flows in each bin to be greater for sub-daily flow data than daily-averaged data, when a fixed number of arithmetically sized bins is used. Because Q_{Eff} was calculated as the median discharge of the bin that produces the maximum sediment yield, $Q_{Eff\text{-}Sub}$ was likely to be greater than $Q_{Eff\text{-}Daily}$ when the same bin was identified as containing Q_{Eff}. This type of error is depicted in Figure 13.

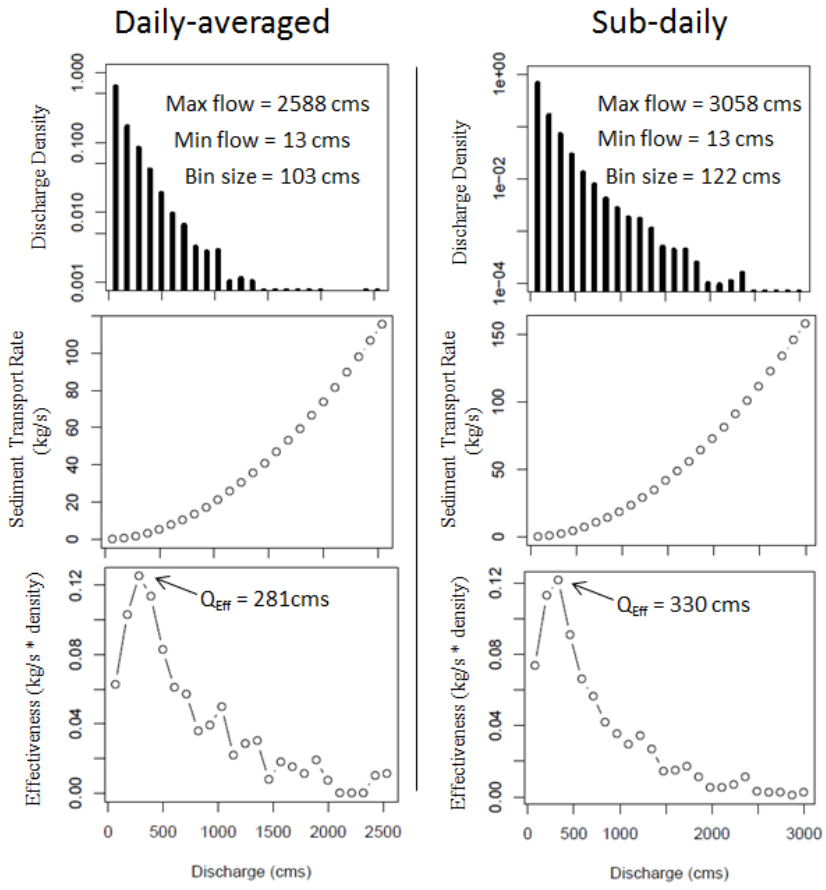

Figure 13: Type A error for the Trinity River near Hoopa, CA. Differences in bin sizes cause disparity in Q_{Eff}, even when the same bin is identified as most effective.

In the case of $Q_{Eff\text{-}Daily}$ / $Q_{Eff\text{-}Sub}$ values greater than unity, differences in flow frequency were found to be the primary cause. We termed this a Type B error. After being multiplied by the sediment rating curve, differences in the frequency of high magnitude discharges between the sub-daily and daily-averaged flow records often caused Q_{Eff} to be located in different bins, thereby causing larger departures in Q_{Eff}. At high discharges, these differences in flow frequency could be very small and still cause large differences in Q_{Eff} when the sediment transport rate at that discharge was particularly high. This was a common result for flashy (RB > 0.3) bedload sites. An example of this type of error is shown in Figure 14.

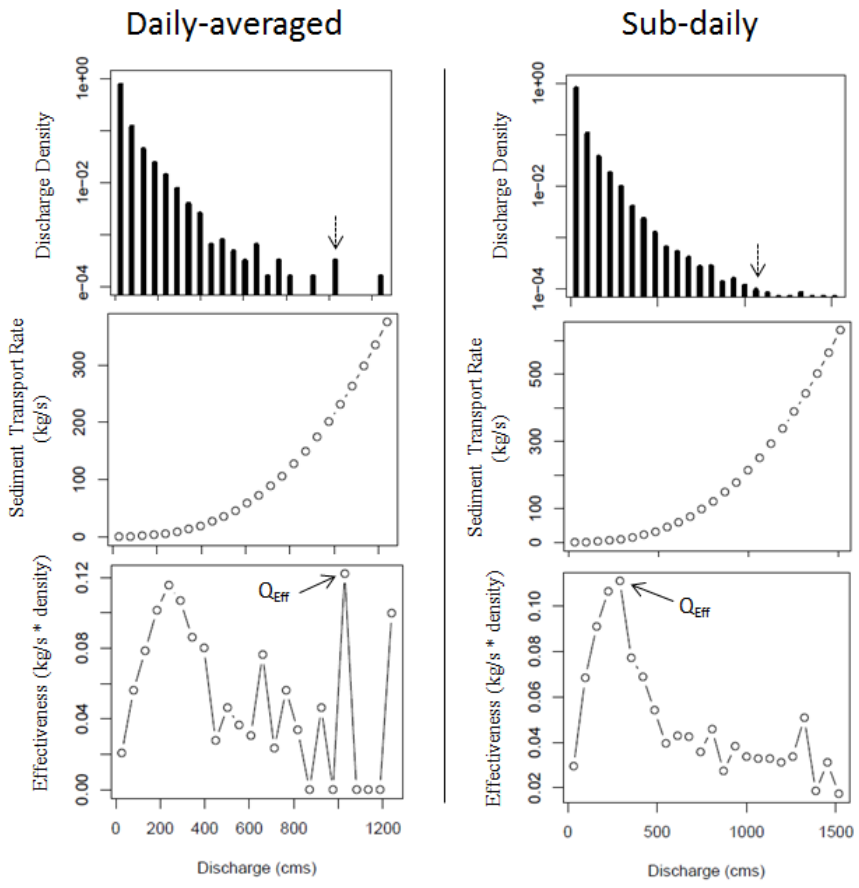

Figure 14: Type B error for the Mad River near Arcata, CA. Differences in discharge density (indicated by dashed arrows) caused the effective discharge to be located in different bins.

As flashiness increases, the sub-daily flow record departs from the daily-average flow record. This causes Type A and Type B errors to become more prevalent and of greater magnitude. This result is seen in Figure 9 where the departure of $Q_{Eff\text{-}Daily}$ / $Q_{Eff\text{-}Sub}$ from 1 was observed to increase with increasing flashiness.

These results indicate that Q_{Eff} is very sensitive to the binning method used, the size of individual bins, and slight differences in flow frequency. In this analysis we computed Q_{Eff} using 25 arithmetic bins as suggested by Biedenharn et al., (2000). The results of this analysis are a direct product of the binning method utilized. Other binning methods have been explored for the computation of Q_{Eff} including the use of arithmetic and logarithmic class intervals and a variable (8-54) number of bins (Soar and Thorne, 2001). It is possible that other binning methods may yield different results than those produced in this analysis.

Comparatively, the half-load discharge (Q_{s50}) was found to be much more stable and easy to compute than Q_{Eff}. Additionally, recent work suggests that Q_{s50} may perform better than Q_{Eff} in the prediction of bankfull discharge for fine bed streams (Sholtes and Bledsoe, 2015, in review). Therefore, we suggest that for certain applications, such as channel design, Q_{s50} may be a more useful metric than Q_{Eff}.

3.4.2 SEDIMENT YIELD and Q_{s50}

Daily-averaged flow data were found to be inadequate in representing the daily hydrograph at flashy sites. Under these circumstances, high sediment-transporting flow rates were diminished by low flows in the averaging process, ultimately causing an underestimation of sediment transport. Sediment yield and Q_{s50} values computed with daily-averaged flow data were both found to differ by varying degrees from values calculated from sub-daily flow data. The

primary control on how SY_{Daily} and $Q_{s50\text{-}Daily}$ varied from SY_{Sub} and $Q_{s50\text{-}Sub}$ was flashiness. Non-flashy systems had SY_{Daily} and $Q_{s50\text{-}Daily}$ values that were very similar to SY_{Sub} and $Q_{s50\text{-}Sub}$. Sediment rating curve parameter *b*, was found to be an important secondary control on the ratio of SY_{Daily}/SY_{Sub} and $Q_{s50\text{-}Daily}/Q_{s50\text{-}Sub}$.

3.4.3 ESTIMATING ERROR IN SEDIENT YIELD AND HALF LOAD DISCHARGE CALCULATIONS

Using the 2-variable interaction model developed through linear regression (Table 10), we can quantitatively describe the difference in *SY* and Q_{s50} values resulting from daily-averaged flow data from values obtained with sub-daily flow data. Because estimates made with sub-daily flow data have greater fidelity to actual physical processes, we can consider differences between sub-daily and daily values of *SY* and Q_{s50} to be errors that depend on *RB* and *b* (Figure 15 and Figure 16).

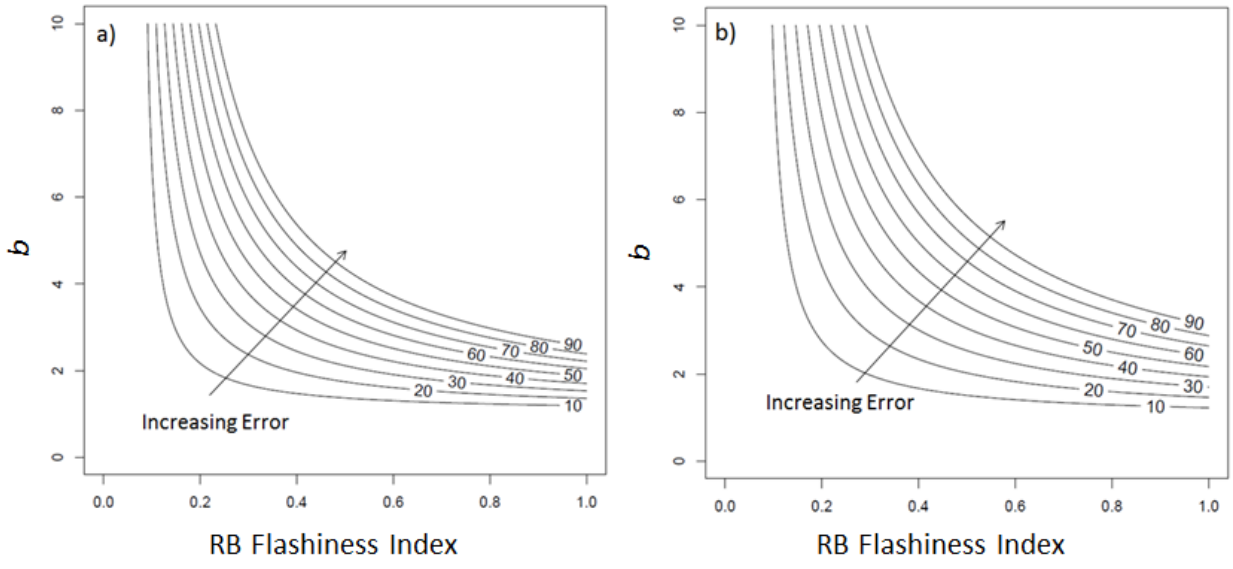

Figure 15: Percent error in sediment yield (*SY*) (values labeled at the top of contours) calculated with daily-averaged flow data. a) bedload sites b) suspended load sites

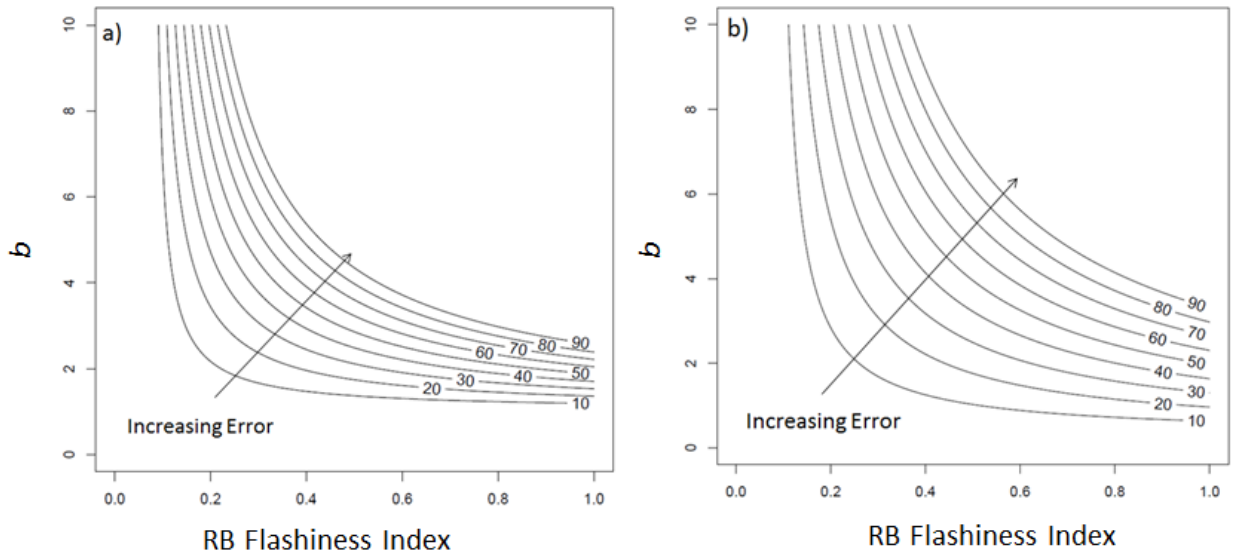

Figure 16: Percent error in half-load discharge (Q_{s50}) (values labeled at the top of contours) calculated with daily-averaged flow data. a) bedload sites b) suspended load sites.

Because the degree of error in *SY* and Q_{s50} computed with daily-averaged flow data depends heavily on *b*, it is important to have a reliable method for estimating *b*. The logarithmic slope of the sediment transport function, *b*, represents a number of physical watershed characteristics including the erosive power of the river and the extent to which new sediment sources become available as discharge increases (Asselman, 2000). The parameter *b* can be most reliably estimated by using a series of sediment discharge measurements and corresponding flow rates to create a best-fit rating curve. Because existing sediment discharge measurements, especially bedload measurements, are few and far between and because collection of new measurements can be cost-prohibitive, this may not be possible. With channel geometry and slope measurements, one may use a total load equation (e.g., Bagnold, 1966; Brownlie, 1981; Einstein, 1950; Yang, 1973) to estimate sediment transport as a function of discharge, from which *b* can be determined. Without measurements of sediment transport, or an understanding of local channel geometry, one may have to rely on a regression equation in order to estimate *b*. In this circumstance, regression equations developed for localized conditions are generally best, but

when these are not available, more global regression equations may be acceptable (Syvitski et al., 2000).

3.4.4 IMPLICATIONS FOR DESIGN OF CHANNEL BED SLOPE

Sediment yield calculations in a flashy system ($RB > 0.4$) with a moderate to large b value ($b > 2$) using daily-averaged flow data are at risk of greatly underestimating sediment yield. In order to quantify the potential effect of underestimating sediment yield on design, we use Henderson proportionalities (Henderson, 1966) to explore how channel design slope may differ when using daily-averaged or sub-daily flow data. Henderson (1966) combined the Einstein sediment transport function as revised by Brown (1950), the Chezy flow resistance formula, and momentum and mass conservation for steady uniform flow into a single proportionality where q_s is the unit sediment transport rate, q is the unit water discharge, S is the channel slope, and D is the grain size.

$$q_s \propto \frac{q^2 S^2}{D^{\frac{3}{2}}} \tag{11}$$

Rearranging for channel slope yields:

$$S \propto \sqrt{\frac{D^{\frac{3}{2}} q_s}{q^2}} \tag{12}$$

Comparing a slope resulting from daily-averaged discharges to one resulting from sub-daily discharges yields:

$$\frac{S_{Daily}}{S_{Sub}} \propto \frac{\sqrt{\frac{D^{\frac{3}{2}} q_{s-Daily}}{q_{Daily}^2}}}{\sqrt{\frac{D^{\frac{3}{2}} q_{s-Sub}}{q_{Sub}^2}}} \tag{13}$$

Wilcock (2004) suggested that the generic form of the relationship in Equation 13 could be used to check for the potential aggradation or degradation of a channel. A ratio of $\frac{S_{Daily}}{S_{Sub}}$ that is less than 1 suggests that use of daily-averaged flow data may result in a bed slope (S_{Daily}) that is too low, thus creating potential for channel aggradation. Likewise, if the ratio of $\frac{S_{Daily}}{S_{Sub}}$ is greater than 1, S_{Daily} may be overestimated, creating potential for channel degradation.

For our purposes, we can assume that bed sediment size remains constant and simplify, yielding:

$$\frac{S_{Daily}}{S_{Sub}} \propto \sqrt{\frac{q_{s-Daily}}{q_{s-Sub}}} * \left(\frac{q_{Daily}}{q_{Sub}}\right)^{-1} \tag{14}$$

Using Q_{s50} as a surrogate for q (both are measures of discharge), and the sediment transport rate associated with Q_{s50} from our sediment rating curve yields:

$$\frac{S_{Daily}}{S_{Sub}} \propto \sqrt{\frac{a * Q_{s50-Daily}{}^{b}}{a * Q_{s50-Sub}{}^{b}}} * \left(\frac{Q_{s50-Daily}}{Q_{s50-Sub}}\right)^{-1} \tag{15}$$

which simplifies to:

$$\frac{S_{Daily}}{S_{Sub}} \propto \left(\frac{Q_{s50-Daily}}{Q_{s50-Sub}}\right)^{\frac{b}{2}-1} \tag{16}$$

Using Equation 16, we can plot the amount by which a design slope calculated using daily-average flow data, S_{Daily}, differs from the design slope calculated with sub-daily flow data, S_{Sub}, which is presumed to be closer to the equilibrium slope (Figure 17). One can see in Figure 17 that for both bedload and suspended load sites, high flashiness and high *b* values correspond to low values of $\frac{S_{Daily}}{S_{Sub}}$. This indicates that using daily-averaged flow data in these types of conditions would result in a channel design slope that is greatly underestimated. An

underestimation of channel design slope can lead to channel aggradation. Conversely, for both suspended load and bedload sites there exist certain combinations of flashiness and *b* that cause $\frac{S_{Daily}}{S_{Sub}}$ to exceed 1. These are areas with a *RB* flashiness less than 0.1 and a *b* greater than 4 (an unlikely combination). For suspended load sites, these are also areas with a *RB* flashiness greater than 0.8 and *b* near 1 (also unlikely). In these cases, daily-averaged flow data causes an over-estimation of channel design slope. This situation could potentially cause channel degradation.

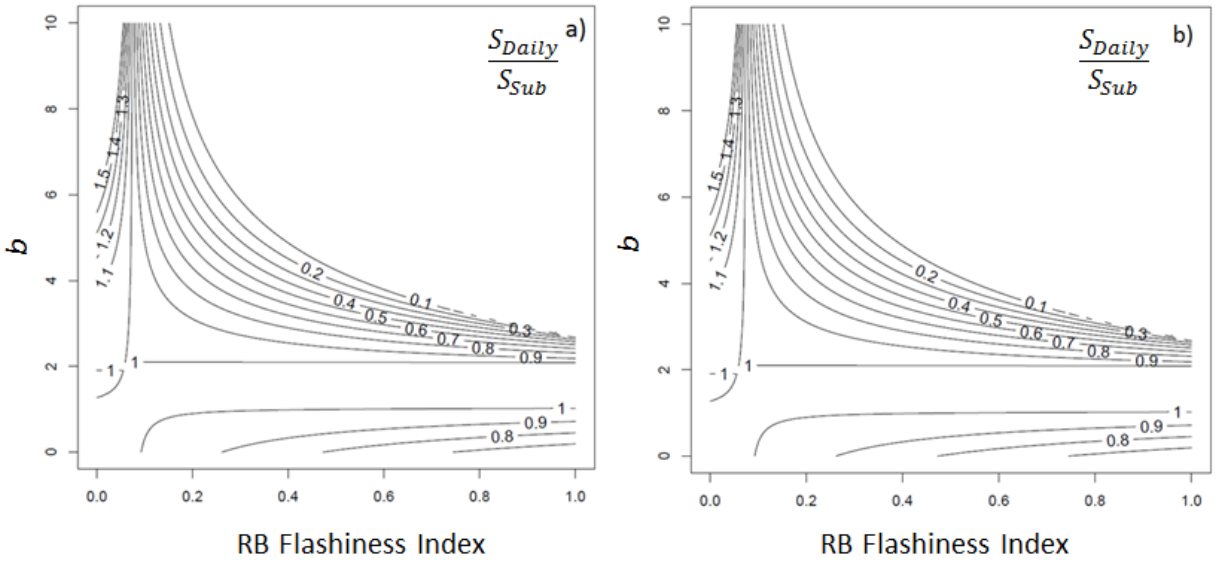

Figure 17: Ratio of design slope calculated with daily flow data (S_{Daily}) to the design slope calculated with sub-daily flow data (S_{Sub}): a) bedload sites b) suspended load sites

3.5 CONCLUSIONS

Our analysis of the effects of flow data resolution on sediment transport calculations for 39 bed load sites and 99 suspended load sites suggests that the use of daily-averaged flow data is not always appropriate. Stream flashiness, and the logarithmic slope of the sediment rating curve, *b*, were found to exhibit strong control on the error created by using daily-averaged flow data in *SY* and Q_{s50} calculations. In instances where the flow regime at the site is flashy (*RB* > 0.4) and

the logarithmic slope of sediment transport is greater than two ($b > 2$), *SY* and Q_{s50} were greatly underestimated using daily-averaged flow data. This underestimation of *SY* and Q_{s50} may then lead to underestimation in channel design slope, which could ultimately cause channel aggradation. Additionally, even in instances where flashiness was high, low logarithmic sediment rating curve slope ($b \approx 1$) controlled the magnitude of error in sediment yield and Q_{s50} calculations, causing error to be quite small. Based on these results, we recommend using sub-daily discharge data for sediment transport calculations when the site either has a *RB* flashiness greater than 0.4 or *b* is greater than 2. Following this recommendation will help keep the error of metrics (*SY*, Q_{s50}, *S*) computed with daily-averaged flow data less than 20% when compared to the same metrics computed with sub-daily flow data.

The decision to use either daily-averaged flow data or sub-daily data does not have a consistent impact on Q_{Eff}. Instances in which $Q_{Eff\text{-}Daily}$ was greater than $Q_{Eff\text{-}Sub}$ were primarily caused by slight differences in flow frequency. Additionally, situations in which $Q_{Eff\text{-}Daily}$ was smaller than $Q_{Eff\text{-}Sub}$ were primarily caused by differences in bin sizes resulting from the sub-daily flow record having a larger range of discharges. Different binning methods may potentially give very different results as Q_{Eff} was found to be very sensitive to bin size and spacing. For this reason, we purpose using the half-load discharge (Q_{s50}) in place of Q_{Eff} as a hydrologic design metric.

3.6 NOTATION

a = sediment rating curve best fit coefficient
b = sediment rating curve best fit exponent, logarithmic slope of sediment transport
BCF = bias correction factor
d_{50} = median grain size (mm)
d_{84} = 84th percentile grain size (mm)
D_{Daily} = Grain size computed from daily flow data

D_{Sub} = Grain size computed from sub-daily flow data
p = probability of rejecting the null hypothesis when the null hypothesis is true
Q_{Eff} = effective discharge $\left(\frac{m^3}{s}\right)$
$Q_{Eff-Daily}$ = effective discharge computed with daily-averaged flow data $\left(\frac{m^3}{s}\right)$
$Q_{Eff-Sub}$ = effective discharge computed with sub-daily flow data $\left(\frac{m^3}{s}\right)$
Q_{s50} = discharge below which 50% of sediment is transported $\left(\frac{m^3}{s}\right)$
$Q_{s50-Daily}$ = discharge below which 50% of sediment is transported, computed from daily flow data $\left(\frac{m^3}{s}\right)$
$Q_{s50-Sub}$ = discharge below which 50% of sediment is transported, computed from sub-daily flow data $\left(\frac{m^3}{s}\right)$
RB = Richards-Baker Flashiness Index (Baker et al., 2004)
S_{Daily} = Design slope computed from daily flow data
S_{Sub} = Design slope computed from sub-daily flow data
SY = Sediment yield
SY_{Daily} = Sediment yield computed with daily flow data
SY_{Sub} = Sediment yield computed with sub-daily flow data
T_{qmean} = the fraction of the time that mean discharge was exceeded

3.7 REFERENCES

Ågren, A., Buffam, I., Jansson, M., & Laudon, H. (2007). Importance of seasonality and small streams for the landscape regulation of dissolved organic carbon export. *Journal of Geophysical Research: Biogeosciences*, 112(3).

Allan, J. D., & Castillo, M. M. (2007). *Stream Ecology: Structure and Function of Running Waters*. Springer Science & Business Media.

Andrews, E. D. (1980). Effective and bankfull discharges of streams in the Yampa River basin, Colorado and Wyoming. *Journal of Hydrology*, 46(3), 311-330.

Asselman, N. E. M. (2000). Fitting and interpretation of sediment rating curves. *Journal of Hydrology*, 234(3), 228-248.

Bagnold, R.A. (1966). An approach to the sediment transport problem from general physics. Professional Paper 422-I. U.S. Geological Survey, Washington, D.C.

Baker, D. B., Richards, R. P., Loftus, T. T., & Kramer, J. W. (2004). A new flashiness index: characteristics and applications to Midwestern rivers and streams. *Journal of the American Water Resources Association*, 40(2), 503-522.

Barry, J. J., Buffington, J. M., & King, J. G. (2004). A general power equation for predicting bed load transport rates in gravel bed rivers. *Water Resources Research*, 40(10).

Biedenharn, D. S., Copeland, R. R., Thorne, C. R., Soar, P. J., Hey, R. D., and Watson, C. C. 2000. "Effective discharge calculation: A practical guide." Technical Rep. No. ERDC/CHL TR-00-15, U.S. Army Corps of Engineers, Washington, D.C.

Brown, C. B. (1950). Sediment transportation. In *Engineering hydraulics*, ed. H. Rouse. New York: Wiley. pp. 769-857.

Brownlie, W.R. (1981). Prediction of flow depth and sediment discharge in open–channels. Report no. KH-R-43A. Pasadena: California Institute of Technology, W.M. Keck Laboratory.

Cade, B. S., & Noon, B. R. (2003). A gentle introduction to quantile regression for ecologists. *Frontiers in Ecology and the Environment*, 1(8), 412-420.

Colby, B. R. (1956). *Relationship of sediment discharge to streamflow*. Open File Rep., U.S. Geological Survey, Water Resources Division, Washington, D.C.

Doyle, M. W., Shields, D., Boyd, K. F., Skidmore, P. B., & Dominick, D. (2007). Channel-forming discharge selection in river restoration design. *Journal of Hydraulic Engineering*, 133(7), 831-837

Dubler, D. (1997). Effective Discharge Determination in the Yazoo River Basin, Mississippi. Masters Thesis, Colorado State University, Department of Civil and Environmental Engineering, Fort Collins, CO.

Einstein, H.A. (1950). The bed load function for sediment transport in open channel flows. Technical Bulletin no. 1026. Washington, D.C.: U.S. Department of Agriculture, Soil Conservation Service.

Emmett, W. W., & Wolman, M. G. (2001). Effective discharge and gravel-bed rivers. *Earth Surface Processes and Landforms*, 26(13), 1369-1380.

Ferguson, R. I. (1987). Accuracy and precision of methods for estimating river loads. *Earth surface processes and landforms*, 12(1), 95-104.

Graf, W. L. (1977). Network characteristics in suburbanizing streams. *Water Resources Research*, 13(2), 459-463.

Henderson, F. M. (1996). *Open channel flow*. Macmillan.

Hendon, S. (1995). Comparison of 15-Minute Versus Mean Daily Flow Duration Curves From The Yazoo Basin, MS. Masters Thesis, Colorado State University, Department of Civil and Environmental Engineering, Fort Collins, CO.

Koenker, R., & Bassett Jr, G. (1978). Regression quantiles. *Econometrica: Journal of the Econometric Society*, 46, 33-50.

Konrad, C. P., & Booth, D. B. (2002). *Hydrologic trends associated with urban development for selected streams in the Puget Sound Basin, western Washington*. United States Geological Survey Water-Resources Investigations Report 02–4040, Tacoma, Washington.

Milliman, J. D., & Meade, R. H. (1983). World-wide delivery of river sediment to the oceans. *The Journal of Geology*, 91, 1-21.

Olson, S. A., and J. M. Norris. (2007). U.S. Geological Survey streamgaging. Fact Sheet 2005-3131. National Streamflow Information Program. Reston, VA: U.S. Geological Survey.

PRISM Climate Group, Oregon State University, http://prism.oregonstate.edu, created 1 Jan 2015.

R Core Team (2014), *R: A Language and Environment for Statistical Computing*, R Foundation for Statistical Computing. Vienna, Austria.

Sholtes, J.S. (2015). On the magnitude and frequency of sediment transport in rivers. Doctoral dissertation. Colorado State University, Department of Civil and Environmental Engineering, Fort Collins, CO.

Sholtes, J.S., and Bledsoe, B.P. (In Review). The half-yield discharge: a process-based predictor of bankfull discharge. *Journal of Hydraulic Engineering*.

Simon, A. 1989. The discharge of sediment in channelized alluvial streams. *Water Resources Bulletin,* 25:1177–1188.

Skidmore, P. B., Shields, F. D., Doyle, M. W., & Miller, D. E. (2001). A categorization of approaches to natural channel design. Proc., *Wetlands Engineering and River Restoration Conference 2001,* ASCE, Reston, VA.

Soar, P. J., and Thorne, C. R. (2001). Channel restoration design for meandering rivers. *Rep. No. ERDC/CHL CR-01-1*, U.S. Army Engineer Research and Development Center, Vicksburg, Miss.

Syvitski, J. P., & Morehead, M. D. (1999). Estimating river-sediment discharge to the ocean: application to the Eel margin, northern California. *Marine Geology*, 154(1), 13-28.

Syvitski, J. P., Morehead, M. D., Bahr, D. B., & Mulder, T. (2000). Estimating fluvial sediment transport: the rating parameters. *Water Resources Research*, 36(9), 2747-2760.

Vogel, R. M., Yaindl, C., & Walter, M. (2011). Nonstationarity: flood magnification and recurrence reduction factors in the United States. *Journal of the American Water Resources Association,* 47, 464-474.

Walling, D. E. (1977). Limitations of the rating curve technique for estimating suspended sediment loads, with particular reference to British rivers. *Erosion and solid matter transport in inland waters,* IAHS Publ. 122:34-48.

Walsh, C. J., Roy, A. H., Feminella, J. W., Cottingham, P. D., Groffman, P. M., & Morgan, R. P. (2005). The urban stream syndrome: current knowledge and the search for a cure. *Journal of the North American Benthological Society*, 24(3), 706-723.

Wheatcroft, R. A., & Sommerfield, C. K. (2005). River sediment flux and shelf sediment accumulation rates on the Pacific Northwest margin. *Continental Shelf Research*, 25(3), 311-332.

Wilcock, P.R. (2004). Sediment transport in the restoration of gravel-bed rivers. *ASCE Conference Proceedings*, 138: 433.

Yang, C. T. (1973). Incipient motion and sediment transport. *Journal of the Hydraulics Division*, *99*(10), 1679-1704.

4 CHAPTER 4: CONCLUSIONS

Urbanization can markedly alter watershed hydrologic response. Changes in the magnitude, frequency, and the rate of change of discharges can have implications on channel morphology and design parameters. In this paper, we developed a case study of how urbanization impacts watershed hydrologic processes for small streams in the Puget Sound region of Washington State. The purpose of this analysis was (i) to tabulate urbanization growth in the selected watersheds; (ii) to evaluate precipitation trends over the analysis period; (iii) to quantify the effects of urbanization on FDCs and stream flashiness; (iv) to relate changes in hydrology to potential changes in channel morphology.

FDC magnitude and stream flashiness increased significantly in urban watersheds. Three of the four urban watersheds were found to have statistically-significant increasing trends over time in both the lower and higher regions of the FDC. For these watersheds, the average increase in the magnitude of high discharges (98^{th} and 99^{th} percentile) was 35% and the average increase in the magnitude of low discharges (10^{th} percentile) was 13%. These results are not suspected to be due to changes in precipitation as no significant trends in annual precipitation totals were found. Results of this analysis also showed that stream flashiness was increasing in nearly all watersheds. In the urban watersheds this result was primarily attributed to increases in impervious surfaces. In rural watersheds this result was attributed to increases in precipitation intensity and variability as well as reductions in baseflow.

From our case study analysis of the effects of urbanization on watershed hydrology, we demonstrate that urbanization can cause dramatic increases in stream flashiness. With the rate at which streamflow changes becoming greater, one might ask at what point do sub-daily flow data become necessary for characterizing the hydrograph. In the third chapter of this paper, we

address this question through an analysis of the effect of flow data resolution on sediment yield estimation.

Choice of flow data resolution is an important consideration in calculation of sediment yield metrics. The degree of stream flashiness, as well as the logarithmic slope of the sediment rating curve, *b*, were found to exhibit strong control on the accuracy of calculations of sediment yield (*SY*) and half load discharge (Q_{s50}). Use of daily-averaged flow data was found to cause an underestimation of *SY* and Q_{s50} in flashy systems. Through this analysis, tools were produced to help quantify the underestimation of these parameters that will result from using daily-averaged flow data as a function of stream flashiness and logarithmic sediment slope, *b*.

4.1 IMPLICATIONS

The results of this research show that urbanization has the potential to cause substantial hydrologic alteration. Through the case study of basins in the Puget Sound, it was observed that urbanization caused increases in FDC magnitude and stream flashiness. Implications of this research are considerable. In urbanizing basins, care should be taken to determine the future potential for FDC shift prior to hydrologic design. For watersheds with a high flashiness, flow data resolution was also shown to be an important consideration in hydrologic design. Daily-averaged flow data do not adequately represent the magnitude of high streamflows at flashy sites. This causes an underestimation of sediment transport and sediment yield at flashy sites, the degree of which is controlled by the magnitude of the best fit exponent of the sediment rating curve. Therefore, when performing sediment yield calculations, it is recommended that sub-daily flow data be used to characterize the hydrograph in flashy watersheds ($RB > 0.4$).

In this paper we have provided plots for estimating error in *SY* and Q_{s50} as a function of *RB* and *b*, when daily-averaged flow data is used (Figure 15 and Figure 16). We have also provided plots that detail the error in channel bed slope that may result from using daily-averaged flow data in the calculation of *SY* and Q_{s50} (Figure 16). By determining the *RB* flashiness index and logarithmic sediment rating curve slope (*b*) at you site, you can quickly use the error plots provided to estimate the error associated with using daily-averaged flow data. This can be used to help inform your choice of daily-averaged or sub-daily flow data. These plots may also be helpful in the correction of sediment yield calculation for instances in which daily-averaged flow data is the only streamflow data available.

5 APPENDIX A

Table 11: Five nearest national climatic center daily precipitation gages to each watershed and their distance.

	First		Second		Third		Fourth		Fifth	
Watershed	Rain gage #	Distance (km)	Rain gage #	Distance (km)	Rain gage #	Distance (km)	Rain gage #	Distance (km)	Rain gage #	Distance (km)
Juanita Creek	USC00455525	30.12	USW00024222	32.18	USW00024234	33.91	USC00452675	42.03	USW00024233	47.45
Mercer Creek	USW00024234	14.29	USW00024233	22.16	USC00454169	22.64	USC00457773	25.08	USC00455525	28.57
Swamp Creek	USW00024222	12.97	USC00452675	25.16	USC00455525	30.19	USW00024234	49.89	USW00024233	64.13
Big Beef Creek	USC00450872	16.25	USC00456846	36.99	USC00459021	39.48	USC00451414	58.78	USW00024234	59.08
Huge Creek	USC00459021	9.09	USC00450872	23.34	USW00024233	43.79	USW00024234	48.22	USC00454169	51.53
Newaukum Creek	USC00450945	6.70	USC00455704	10.42	USC00456295	13.30	USC00454486	16.54	USC00455224	22.82
Issaquah Creek	USC00454486	12.53	USC00457773	13.43	USC00451233	19.73	USC00454169	20.22	USC00456295	22.90
Leach Creek	USC00459021	20.14	USC00455224	23.06	USW00024233	27.08	USC00454169	28.25	USW00024234	35.82

6 APPENDIX B

Table 12: Bedload sites used in the analysis of the effect of flow data resolution on sediment yield metrics.

Site.Number	Location	Drainage Area (km^2)	Gage Elevation (m)	Latitude	Longitude	RB Flash	d50 (mm)	d85 (mm)	a	b	BCF
11173575	Alameda Creek below Welch Creek near Sunol, CA	386	91	37.541	-121.855	0.366	14.7	35.5	1.29E-04	1.40	2.13
11179000	Alameda Creek near Niles, CA	1,639	26	37.587	-121.960	0.445	5.31	15.9	2.15E-05	1.95	1.58
13120500	Big Lost River at Howell Ranch near Chilly, ID	1,139	2018	43.998	-114.021	0.101	NA	NA	5.00E-05	2.53	2.00
13185000	Boise River near Twin Springs, ID	2,154	1018	43.668	-115.725	0.091	70	141	4.37E-06	2.64	1.23
13018300	Cache Creek near Jackson, WY	17,476	2057	43.452	-110.703	0.050	46	115	6.21E-04	2.65	1.22
11143250	Carmel River near Carmel, CA	639	12	36.539	-121.879	0.269	8.34	18.5	7.32E-04	1.58	2.02
13342500	Clearwater River at Spalding, ID	24,034	235	46.449	-116.826	0.085	74	NA	2.80E-07	2.20	1.44
09339900	East Fork San Juan River, CO	166	2420	37.390	-106.841	0.102	49	112	3.77E-06	5.14	1.19
09404900	East Fork Virgin River near Springdale, UT	10,201	1201	37.164	-112.958	0.098	25	NA	2.38E-03	0.97	1.24
12044900	Elwha River Above Lake Mills near Port Angeles, WA	513	0	47.970	-123.589	0.178	NA	NA	6.85E-04	2.34	1.56
07083000	Halfmoon Creek near Malta, CO	61	2996	39.172	-106.389	0.093	49	119	1.77E-04	3.33	1.73
11525670	Indian Creek near Douglas City, CA	87	518	40.652	-122.913	0.177	NA	NA	5.12E-06	2.87	1.47
13162225	Jarbidge River below Jarbridge, NV	79	1844	41.891	-115.428	0.126	91	164	1.97E-04	3.07	2.37
13313000	Johnson Creek at Yellow Pine, ID	564	1419	44.962	-115.500	0.092	190	380	4.56E-07	2.90	1.31
13310660	Little Buckhorn Creek near Krassel Ranger Station, ID	16	1265	44.913	-115.750	0.073	66	240	2.40E-02	2.13	1.65

13019438	Little Granite Creek at mouth near Bondurant, WY	55	1948	43.299	-110.518	0.076	154.5	NA	2.41E-04	2.94	2.40
13337000	Lochsa River near Lowell, ID	3,050	443	46.151	-115.587	0.099	131	275	1.83E-11	3.99	1.47
13309220	Middle Fork Salmon River at Middle Fork Lodge near Yellow Pine, Idaho	2,698	1335	44.722	-115.016	0.084	134	290	4.97E-16	6.39	1.71
11148900	Nacimiento River below Sapaque Creek near Bryson, CA	419	244	35.789	-121.093	0.601	77.5	NA	1.36E-06	2.49	1.41
13340600	North Fork Clearwater River near Canyon Ranger Station, ID	3,355	506	46.841	-115.621	0.096	86	210	3.44E-11	3.92	1.31
13011500	Pacific Creek at Moran, WY	438	2048	43.850	-110.518	0.114	78.5	NA	1.71E-04	2.39	2.96
11482500	Redwood Creek at Orick, CA	717	2	41.299	-124.050	0.280	6.61	19.3	1.73E-04	1.34	1.22
11481500	Redwood Creek near Blue Lake, CA	175	259	40.906	-123.814	0.280	21.9	44	9.21E-06	2.46	1.46
11525530	Rush Creek Near Lewiston, CA	58	560	40.725	-122.834	0.202	NA	NA	3.27E-06	3.11	1.74
10343500	Sagehen Creek near Truckee, CA	27	1926	39.432	-120.237	0.118	58	NA	6.29E-03	1.57	1.96
13296500	Salmon River below Yankee Fork near Clayton, ID	2,089	1798	44.268	-114.733	0.063	104	280	3.68E-09	3.87	1.61
13307000	Salmon River near Shoup, ID	16,153	961	45.323	-114.440	0.056	96	173	3.01E-10	3.87	1.39
11149900	San Antonio River near Lockwood, CA	562	961	35.897	-121.087	0.399	4.55	14.6	4.47E-03	0.82	1.46
11254000	San Joaquin River near Mendota, CA	10,201	43	36.811	-120.377	0.072	0.73	1.58	5.10E-05	1.06	1.47
13336500	Selway River near Lowell, ID	4,958	469	46.087	-115.514	0.098	182	278	8.75E-14	4.81	1.41
13310700	South Fork Salmon River near Krassel Ranger Station, ID	9,709	1143	44.987	-115.725	0.098	14	75	2.29E-06	3.01	2.32
13235000	South Fork Payette River at Lowman, ID	1,155	1155	44.085	-115.622	0.071	95	210	1.13E-04	2.13	1.35
13297355	Squaw Creek near Clayton, ID	185	1740	44.291	-114.472	0.091	46	91	1.32E-03	2.40	2.10

13297330	Thompson Creek near Clayton, ID	75	1737	44.270	-114.517	0.091	63	120	3.02E-03	2.99	1.28
11525854	Trinity River at Douglas City, CA	2,410	487	40.645	-122.957	0.077	NA	NA	5.50E-09	2.98	1.26
13295000	Valley Creek at Stanley, ID	381	1893	44.223	-114.931	0.081	63	160	9.08E-05	2.66	2.13
09415000	Virgin River at Littlefield, AZ	13,178	538	36.892	-113.924	0.207	0.31	0.54	5.57E-03	0.43	1.34
13310670	West Fork Buckhorn Creek near Krassel Ranger Station, ID	59	1262	44.917	-115.743	0.109	180	510	1.59E-03	1.75	2.21
06228000	Wind River at Riverton, WY	5,978	1494	43.011	-108.376	0.155	22.00	40.00	8.30E-03	1.18	1.21

Table 13: Suspended load sites used in the analysis of flow data resolution's effect on sediment yield metrics.

Suspended Load Sites											
USGS Site Number	Location	Drainage Area (km^2)	Gage Elevation (m)	Latitude	Longitude	RB Flash	d50 (mm)	d85 (mm)	a	b	BCF
09364500	Animas River at Farmington, NM	3,521	415	36.723	-108.202	0.106	0.286	32	6.81E-05	2.12	4.51
07146500	Arkansas River at Arkansas City, KS	113,173	329	37.056	-97.058	0.254	0.4265	2	2.27E-05	1.96	2.32
07152500	Arkansas River at Ralston, OK	120,728	237	36.504	-96.728	0.105	0.531	1.92	3.17E-04	1.89	1.93
07164500	Arkansas River at Tulsa, OK	192,777	188	36.141	-96.006	0.202	NA	NA	3.16E-05	1.63	3.14
07137500	Arkansas River near Coolidge, KS	65,786	1015	38.028	-102.011	0.189	NA	NA	4.23E-05	1.28	2.80
08340500	Arroyo Chico near Guadalupe, NM	3,599	1805	35.592	-107.189	0.995	5	12.5	5.28E-02	1.74	2.10
11176900	Arroyo de la Laguna at Verona, CA	1,043	85	37.627	-121.882	0.661	2.905	16.25	9.74E-05	1.99	2.63
11047300	Arroyo Trabuco at San Juan Capistrano, CA	140	24	33.498	-117.665	0.756	NA	NA	2.47E-03	2.15	2.40
07196900	Baron Fork at Dutch Mills, AR	105	301	35.880	-94.486	0.710	NA	NA	2.06E-03	0.97	1.61
07290000	Big Black River near Bovina, MS	7,280	26	32.348	-90.697	0.146	0.38	0.63	9.98E-05	1.18	1.82
06485500	Big Sioux River at Akron, IA	20,399	341	42.838	-96.562	0.114	0.59	1.11	1.27E-04	1.35	1.60
01481500	Brandywine Creek at Wilmington, DE	813	20	39.770	-75.577	0.357	NA	NA	5.66E-06	2.13	1.32
08114000	Brazos River at Richmond, TX	92,016	9	29.582	-95.758	0.134	0.208	0.414	1.04E-07	2.72	2.40
08123850	Colorado River above Silver, TX	38,602	581	32.054	-100.762	0.053	NA	NA	6.89E-07	2.45	1.62

08158000	Colorado River at Austin, TX	100,994	119	30.246	-97.680	0.055	NA	NA	8.95E-08	2.76	1.98
08162000	Colorado River at Wharton, TX	108,746	16	29.309	-96.104	0.054	NA	NA	1.21E-06	2.32	1.94
09095500	Colorado River near Cameo, CO.	20,676	1467	39.239	-108.266	0.640	NA	NA	6.79E-05	1.42	3.10
09180500	Colorado River near Cisco, UT	62,395	1247	38.811	-109.293	0.154	NA	NA	4.83E-05	1.07	2.71
09163500	Colorado River near Colorado-Utah State Line	46,211	1318	39.133	-109.026	0.276	NA	NA	2.16E-06	2.28	2.77
08147000	Colorado River near San Saba, TX	80,821	334	31.218	-98.564	0.414	NA	NA	6.31E-05	1.09	2.46
02075500	Dan River at Paces, VA	6,698	98	36.642	-79.090	0.291	NA	NA	2.17E-06	2.05	2.16
03365500	East Fork White River at Seymour, IN	6,061	168	38.983	-85.899	0.272	1.63	4.4	4.02E-04	0.99	1.50
11475000	Eel River at Fort Seward, CA	5,455	66	40.218	-123.631	0.338	2.93	13.8	3.57E-07	2.50	1.80
11477000	Eel River at Scotia, CA	8,060	11	40.492	-124.099	0.322	NA	NA	2.21E-06	2.16	1.71
09466500	Gila River at Calva, AZ	29,696	767	33.186	-110.219	0.286	NA	NA	7.85E-04	1.95	2.14
09474000	Gila River at Kelvin, AZ	46,630	532	33.103	-110.976	0.136	NA	NA	6.97E-04	1.69	2.84
09431500	Gila River near Redrock, NM	7,324	862	32.727	-108.676	0.259	NA	NA	7.31E-05	2.09	3.48
09315000	Green River at Green River, UT	116,117	1231	38.986	-110.151	0.053	NA	NA	2.21E-08	3.13	2.28
07277700	Hickahala Creek near Senatobia, MS	313	71	34.632	-89.924	0.957	NA	NA	8.16E-05	2.50	1.77
05568800	Indian Creek near Wyoming, IL	162	185	41.019	-89.836	0.390	1	5.6	6.81E-04	1.36	2.13
05454500	Iowa River at Iowa City, IA	8,469	188	41.657	-91.541	0.089	NA	NA	3.42E-06	1.74	2.37
05451500	Iowa River at Marshalltown, IA	3,966	260	42.066	-92.908	0.145	0.4725	1.077	4.25E-05	1.77	2.17

05526000	Iroquois River near Chebanse, IL	5,414	182	41.009	-87.823	0.179	NA	NA	5.33E-05	1.14	1.76
05520500	Kankakee River at Momence, IL	5,939	186	41.160	-87.669	0.061	NA	NA	8.64E-06	1.76	1.74
05591200	Kaskaskia River at Cooks Mills, IL	1,225	188	39.583	-88.413	0.235	0.912	12	1.57E-04	0.99	2.43
05594100	Kaskaskia River near Venedy Station, IL	11,373	116	38.451	-89.628	0.121	0.316	0.5625	6.06E-05	1.20	2.67
11523000	Klamath River at Orleans, CA	21,942	109	41.304	-123.533	0.119	3.575	7.83	9.88E-08	2.50	1.69
11530500	Klamath River near Klamath, CA	31,327	0	41.511	-123.978	0.136	NA	NA	2.90E-08	2.61	1.68
07143672	Little Arkansas River at Highway 50 near Halstead, KS	1,965	418	38.029	-97.540	0.484	NA	NA	1.20E-04	1.45	2.04
07144100	Little Arkansas River near Sedgwick, KS	3,016	408	37.883	-97.424	0.499	0.8625	3.655	4.19E-05	1.57	1.75
03353600	Little Eagle Creek at Speedway, IN	63	216	39.788	-86.229	0.830	NA	NA	1.27E-02	1.05	1.86
09260000	Little Snake River near Lily, CO	10,444	1733	40.549	-108.424	0.122	0.626	1.335	2.20E-03	1.50	3.50
05099400	Little South Pembina River near Walhalla, ND	445	336	48.865	-98.006	0.420	2.4	7.36	4.15E-04	2.05	2.17
03261950	Loramie Creek near Newport, OH	394	282	40.307	-84.384	0.567	0.375	1	1.68E-05	1.74	1.15
11481000	Mad River near Arcata, CA	1,256	4	40.910	-124.059	0.299	NA	NA	2.24E-06	2.62	1.32
04193500	Maumee River at Waterville, OH	16,388	181	41.500	-83.713	0.295	NA	NA	5.54E-07	1.94	5.48
11473900	Middle Fork Eel River near Dos Rios, CA	1,929	275	39.706	-123.324	0.326	NA	NA	1.20E-05	2.20	1.44
05325000	Minnesota River at Mankato, MN	38,576	228	44.169	-94.003	0.073	NA	NA	1.28E-04	1.43	2.30
07374000	Mississippi River at Baton Rouge, LA	2,914,722	0	30.446	-91.192	0.021	NA	NA	3.68E-14	3.43	1.27
05420500	Mississippi River at Clinton, IA	221,618	172	41.781	-90.252	0.046	NA	NA	1.07E-07	1.77	2.04

07022000	Mississippi River at Thebes, IL	1,846,475	91	37.222	-89.463	0.041	0.4385	1.087	2.01E-06	1.73	1.71
05267000	Mississippi River near Royalton, MN	30,032	317	45.826	-94.355	0.057	NA	NA	2.04E-04	0.57	1.69
06088500	Muddy Creek at Vaughn, MT	662	78	47.561	-111.542	0.109	NA	NA	1.93E-04	2.43	1.79
08041000	Neches River at Evadale, TX	20,585	3	30.356	-94.093	0.065	0.23	0.57	1.60E-04	0.99	3.15
04024430	Nemadji River near South Superior, WI	1,087	183	46.633	-92.094	0.353	0.451	0.955	1.40E-05	2.03	1.66
02089500	Neuse River at Kinston, NC	6,970	3	35.258	-77.586	0.104	0.57	0.85	2.25E-05	1.28	1.96
06810000	Nishnabotna River above Hamburg, IA	7,265	273	40.602	-95.645	0.185	NA	NA	1.35E-05	2.16	1.77
06817000	Nodaway River at Clarinda, IA	1,973	291	40.743	-95.014	0.436	0.479	1.27	2.29E-05	2.22	2.18
02047000	Nottoway River near Sebrell, VA	3,731	1	36.770	-77.166	0.178	1.28	2.2	2.17E-05	1.10	2.23
09382000	Paria River at Lees Ferry, AZ	3,650	952	36.872	-111.594	0.521	0.2925	1.75	2.78E-02	2.47	1.91
08407500	Pecos River at Red Bluff, NM	50,589	869	32.075	-104.039	0.156	NA	NA	1.35E-04	1.39	3.25
08396500	Pecos River near Artesia, NM	39,612	1003	32.841	-104.324	0.181	NA	NA	3.85E-04	1.84	1.71
08383500	Pecos River near Puerto de Luna, NM	10,278	1314	34.730	-104.525	0.203	NA	NA	1.81E-04	2.37	3.79
02131000	Pee Dee River at Peedee, SC	22,861	8	34.204	-79.549	0.112	NA	NA	9.02E-05	0.88	1.90
05099600	Pembina River at Walhalla, ND	8,673	284	48.913	-97.917	0.142	0.62	1.37	4.25E-04	1.53	4.07
01653600	Piscataway Creek at Piscataway, MD	102	2	39.706	-76.966	0.634	NA	NA	4.47E-03	1.98	3.06
01668000	Rappahannock River near Fredericksburg, VA	4,129	21	38.308	-77.529	0.417	1.47	7.735	5.50E-07	2.26	2.38
05079000	Red Lake River at Crookston, MN	13,644	254	47.776	-96.609	0.123	NA	NA	2.75E-05	1.24	2.45

07337000	Red River at Index, AR	124,272	75	33.552	-94.041	0.113	NA	NA	3.20E-07	2.42	2.52
05054000	Red River of the North at Fargo, ND	17,605	263	46.861	-96.783	0.089	0.26	0.55	2.08E-05	1.24	1.49
05064500	Red River of the North at Halstad, MN	56,440	252	47.352	-96.843	0.086	NA	NA	6.33E-05	0.98	1.81
11482500	Redwood Creek at Orick CA	717	2	41.299	-124.050	0.280	0.618	3.45	9.64E-06	2.29	1.68
11481500	Redwood Creek near Blue Lake CA	175	259	40.906	-123.814	0.280	5	14.7	1.31E-05	2.73	1.76
08330000	Rio Grande at Albuquerque, NM	37,541	1508	35.089	-106.681	0.078	NA	NA	9.21E-05	2.16	2.46
08313000	Rio Grande at Otowi Bridge, NM	37,023	1673	35.875	-106.142	0.063	0.4565	0.9365	6.19E-04	1.70	3.31
08319000	Rio Grande at San Felipe, NM	41,683	1559	35.445	-106.440	0.056	0.8445	2	1.98E-05	2.03	3.78
08276500	Rio Grande Below Taos Junction Bridge near Taos, NM	17,579	1844	36.320	-105.754	0.056	NA	NA	5.95E-06	2.19	2.31
08354900	Rio Grande Floodway at San Acacia, NM	61,696	1419	34.256	-106.891	0.105	NA	NA	1.54E-03	1.46	7.30
08358400	Rio Grande Floodway at San Marcial, NM	64,104	1358	33.679	-106.997	0.111	NA	NA	5.89E-04	1.93	2.67
08334000	Rio Puerco Above Arroyo Chico near Guadalupe, NM	1,087	1814	35.601	-107.167	0.676	NA	NA	1.13E-01	1.89	1.94
08353000	Rio Puerco near Bernardo, NM	16,104	1439	34.410	-106.854	0.636	NA	NA	3.01E-02	1.76	2.58
09379500	San Juan River near Bluff, UT	59,547	1234	37.147	-109.864	0.807	NA	NA	1.08E-02	1.70	1.39
11042000	San Luis Rey River at Oceanside, CA	1,442	6	33.218	-117.359	0.101	2.6425	9.41	1.61E-04	2.05	3.54
09471000	San Pedro River at Charleston, AZ	3,195	1205	31.626	-110.174	0.373	NA	NA	7.04E-04	1.69	3.77
05572000	Sangamon River at Monticello, IL	1,424	191	40.031	-88.589	0.707	0.4345	0.774	9.87E-03	2.03	1.90
05583000	Sangamon River near Oakford, IL	13,186	138	40.124	-89.985	0.227	0.397	1.09	2.37E-04	1.02	2.27

11113000	Sespe Creek near Fillmore, CA	652	172	34.442	-118.926	0.124	0.494	1.55	7.18E-06	1.84	2.01
01658500	South Fork Quantico Creek near Independent Hill, VA	20	72	38.587	-77.429	0.640	NA	NA	1.40E-04	2.12	2.23
05570000	Spoon River at Seville, IL	4,236	142	40.490	-90.340	0.227	NA	NA	2.21E-04	1.32	1.58
01095220	Stillwater River near Sterling, MA	82	122	42.411	-71.792	0.312	0.455	1.3	4.05E-05	1.28	1.32
01401000	Stony Brook at Princeton, NJ	115	19	40.333	-74.682	0.804	NA	NA	1.47E-05	1.83	1.71
11530000	Trinity River at Hoopa, CA	7,386	84	41.050	-123.673	0.147	NA	NA	3.61E-05	1.89	1.18
08066500	Trinity River at Romayor, TX	44,495	8	30.425	-94.851	0.063	2	13	6.79E-06	1.82	2.45
08062700	Trinity River at Trinidad, TX	22,105	72	32.148	-96.102	0.107	NA	NA	7.87E-07	2.00	3.28
08057410	Trinity River below Dallas, TX	16,254	112	32.708	-96.736	0.180	NA	NA	4.43E-06	1.90	2.79
11525655	Trinity River Below Limekiln Gulch near Douglas City, CA	2,097	503	40.673	-122.919	0.258	NA	NA	1.38E-06	2.04	2.30
07331000	Washita River near Dickson, OK	18,568	198	34.233	-96.976	0.269	0.339	0.923	1.07E-04	1.96	2.50
02217274	Wheeler Creek at Bill Cheek Road, near Auburn, GA	3	270	34.082	-83.855	0.609	0.16	0.21	3.59E-03	1.89	2.33
09251000	Yampa River near Maybell, CO	8,759	1798	40.503	-108.033	0.096	NA	NA	7.02E-06	2.22	1.44